THE JOURNAL OF BIOLOGICAL CHEMISTRY VOL. 287, NO. 53, pp. 44046–44061, December 28, 2012

Kinin-B2 Receptor Activity Determines the Differentiation Fate of Neural Stem Cells*

Received for publication, August 2, 2012, and in revised form, November 5, 2012 Published, JBC Papers in Press, November 6, 2012, DOI 10.1074/jbc.M112.407197

Cleber A. Trujillo[‡1], Priscilla D. Negraes[‡1], Telma T. Schwindt[‡1], Claudiana Lameu[‡], Cassiano Carromeu[§2], Alysson R. Muotri[§3], João B. Pesquero[¶], Débora M. Cerqueira[‖], Micheli M. Pillat[‡4], Héllio D. N. de Souza[‡5], Lauro T. Turaça[¶], José G. Abreu[‖], and Henning Ulrich[‡6]

From the [‡]Departamento de Bioquímica, Instituto de Química, Universidade de São Paulo, São Paulo, Brazil 05508-000, the [§]Departments of Pediatrics and Cellular and Molecular Medicine, University of California at San Diego, San Diego, California 92093, the [¶]Departamento de Biofísica, Universidade Federal de São Paulo, SP, Brazil 04023-062, and the [‖]Instituto de Ciências Biomédicas, Universidade Federal do Rio de Janeiro, Rio de Janeiro, Brazil 21941-902

Background: Recent studies point at functions of bradykinin in the CNS including neuromodulation and neuroprotection.
Results: Bradykinin augments neurogenesis of neural stem cells from embryonic telencephalon, whereas bradykinin receptor inhibition promotes gliogenesis.
Conclusion: Bradykinin acts as switch for phenotype determination using an *in vitro* system of migrating cells, closely reflecting conditions of cortex development.
Significance: Novel functions are described for bradykinin with therapeutic relevance.

Bradykinin is not only important for inflammation and blood pressure regulation, but also involved in neuromodulation and neuroprotection. Here we describe novel functions for bradykinin and the kinin-B2 receptor (B2BkR) in differentiation of neural stem cells. In the presence of the B2BkR antagonist HOE-140 during rat neurosphere differentiation, neuron-specific *β3-tubulin* and *enolase* expression was reduced together with an increase in glial protein expression, indicating that bradykinin-induced receptor activity contributes to neurogenesis. In agreement, HOE-140 affected in the same way expression levels of neural markers during neural differentiation of murine P19 and human iPS cells. Kinin-B1 receptor agonists and antagonists did not affect expression levels of neural markers, suggesting that bradykinin-mediated effects are exclusively mediated via B2BkR. Neurogenesis was augmented by bradykinin in the middle and late stages of the differentiation process. Chronic treatment with HOE-140 diminished *eNOS* and *nNOS* as well as *M1–M4 muscarinic receptor* expression and also affected purinergic receptor expression and activity. Neurogenesis, gliogenesis, and neural migration were altered during differentiation of neurospheres isolated from *B2BkR* knock-out mice. Whole mount *in situ* hybridization revealed the presence of *B2BkR* mRNA throughout the nervous system in mouse embryos, and less *β3-tubulin* and more glial proteins were expressed in developing and adult *B2BkR* knock-out mice brains. As a underlying transcriptional mechanism for neural fate determination, HOE-140 induced up-regulation of *Notch1* and *Stat3* gene expression. Because pharmacological treatments did not affect cell viability and proliferation, we conclude that bradykinin-induced signaling provides a switch for neural fate determination and specification of neurotransmitter receptor expression.

The central nervous system is originated from a monolayer of neuroepithelial cells from which single neural progenitors arise, proliferate, and differentiate into a complex neural network (1–3). One of the most important steps during brain development is the generation of cellular diversity, *i.e.* the decision to form neurons or glial cells. This dynamic process is tightly regulated by spatial and temporal patterns (4, 5). The mechanisms underlying progenitor proliferation and differentiation during development are related to both extrinsic and intrinsic factors (6). Extrinsic factors, including neurotransmitters, cytokines, hormones and growth factors, have been shown to influence the acquisition of neuronal or glial phenotypes (7, 8). These diffusible factors activate membrane-bound receptors, which act as morphogens and regulate the progress of neural differentiation (9).

One factor that may play a role in neural differentiation that has not been previously studied in this context is bradykinin (Bk).[7] Kinins are biologically active peptides released into the

* This work was supported, in whole or in part, by National Institutes of Health Director's New Innovator Award Program Grant 1-DP2-OD006495-01 (to A. R. M.), research grants from Fundação de Amparo à Pesquisa do Estado de São Paulo (FAPESP) (number 2006/61285-9), Conselho Nacional de Desenvolvimento Científico e Tecnológico (CNPq), and the Provost's Office for Research of the University of São Paulo Programa de Incentivo à Pesquisa, Project numbers 2011.1.9333.1.3 and NAPNA-USP, Brazil (to H. U.).
[1] Supported by fellowships from FAPESP.
[2] Supported by a fellowship from the International Rett Syndrome Foundation, 2517.
[3] Supported by the Emerald Foundation and the California Institute for Regenerative Medicine Grant TR2-01814.
[4] Supported by a fellowship from Coordenação de Aperfeiçoamento de Pessoal de Nível Superior (CAPES).
[5] Supported by a fellowship from Conselho Nacional de Desenvolvimento Cientifico e Tecnológico.
[6] To whom correspondence should be addressed: Av. Prof. Lineu Prestes 748, CEP 05508–900, São Paulo, SP, Brazil. Tel.: 55-11-3091-8512; Fax: 55-11-3815-5579; E-mail: henning@iq.usp.br.

[7] The abbreviations used are: Bk, bradykinin; NPC, neural progenitor cell; iPS, induced pluripotent stem; ACE, angiotensin-converting enzyme; ASS, argininosuccinate synthetase; eNOS, endothelial nitric-oxide synthase; nNOS, neuronal nitric-oxide synthase; GFAP, glial fibrillary acidic protein; NO, nitric oxide; CNS, central nervous system.

plasma or interstitial fluid after proteolytic cleavage of kininogens by kallikreins. The kallikrein-kinin system is best known for its involvement in cardiovascular homeostasis, coagulation, inflammation, pain, and development (10–12). Moreover, there are also effects on neuronal physiology of Bk and related kinins (13, 14). B1 (B1BkR) and B2 (B2BkR) G protein-coupled receptors are present in the CNS and participate in many signaling cascades and physiological consequences including NO formation and glutamate release (15–18).

Previously, we have shown that Bk secretion and *B2BkR* expression are regulated during *in vitro* neuronal differentiation of P19 embryonal carcinoma cells. Receptor expression and activity as well as generation of Bk rose with ongoing neuronal differentiation. Carbachol-induced intracellular calcium transients and gene expression of muscarinic receptors were suppressed following chronic treatment of differentiating cells with HOE-140, a specific B2BkR-antagonist (19). Thus, B2BkR activity was essential for differentiation of P19 cells into neurons with a cholinergic phenotype.

Here we report novel functions for Bk in phenotype determination whether a neural progenitor cell (NPC) differentiates into a neuron or a glial cell. Three *in vitro* differentiation models, P19 mouse embryonal carcinoma cells, rat NPCs, and human induced pluripotent stem cells were used to demonstrate the importance of B2BkR in neural fate and neurotransmitter receptor expression determination. As an underlying mechanism, we found that migration of NPCs was largely restricted when B2BkR activity was inhibited. These results were confirmed in migration assays with neurospheres obtained from *B2BkR* knock-out mice, which also revealed reduced migration. We also observed a strong expression of *B2BkR* in the developing mouse brain, and reduced β3-*tubulin* expression in *B2BkR* knock-out embryos. Together, these results indicate a novel function of Bk in the determination of cell fate in the process of neural differentiation.

EXPERIMENTAL PROCEDURES

Animals—This work was approved by the Ethics on Animal Care and Use Committee of the Instituto de Química of the Universidade de São Paulo. Wistar Hannover rats, wild type and *B2BkR*$^{-/-}$ C57BL/6 mice (provided by Instituto de Química and Center for Development of Experimental Models for Medicine and Biology, UNIFESP, respectively), were used for neural progenitor isolation and neurosphere formation. Animals were housed under optimal light, temperature, and humidity conditions, with food and water provided *ad libitum*. Timed-pregnant animals were obtained by overnight mating. The efficiency of mating was confirmed by the presence of sperm after vaginal smear or appearance of the vaginal plug. Comparison of the *B2BkR*$^{-/-}$ mice was made with their wild-type littermates. Following 14 (rats) and 12.5 days (mice) of gestation, females were sacrificed in a chamber with a saturated CO_2 atmosphere. Genotyping of the *B2BkR*$^{-/-}$ mice was performed using polymerase chain reaction (PCR) of genomic DNA extracted from tails. Detailed genotyping procedure and primers for PCR have been previously described (20).

Cortical Primary Culture—Newborn rats were decapitated and their brains removed aseptically in ice-cold phosphate-buffered saline (PBS). Briefly, after removal of meninges, the cerebral cortex was dissected and dissociated by incubation with 0.05% trypsin solution at 37 °C for 5 min followed by light trituration. After cell counting, cells were plated in DMEM/F-12 (Life Technologies) with 10% fetal bovine serum (FBS) at a density of 3×10^5 cells/ml in poly-L-lysine (1 mg/ml) pretreated dishes. The medium was replaced every other day for 7 days, and the cells remained in the incubator at 37 °C with controlled humidity and 5% CO_2.

Neurosphere Culture and Differentiation—NPCs were isolated from telencephalon of E14 rats or E12.5 mice embryos, using techniques previously described (21). After brain dissection, telencephalon was subjected to mechanical and enzymatic dissociation. Cells were grown in suspension at a density of 2×10^5 cells/ml in DMEM/F-12 in the presence of 100 IU/ml of penicillin, 100 μg/ml of streptomycin, 2 mM L-glutamine, 5 μg/ml of heparin, 20 ng/ml of FGF-2, 20 ng/ml of EGF, and 2% B-27 (Life Technologies) at 37 °C in 95% humidity and 5% CO_2. Cultures were grown for 10 days with one passage prior to neural differentiation. For differentiation studies, primary whole neurospheres were allowed to attach to poly-L-lysine and laminin-coated coverslips or culture flasks with DMEM/F-12, 2% B-27 in the absence of FGF-2 and EGF. Progenitor cells were differentiated for 7 days and treated with 1 μM HOE-140 (Tocris Bioscience) or 1 μM Bk (Tocris Bioscience). The migration assay was evaluated on the seventh day of differentiation as the distance of the foremost cells to the neurosphere boundary. Neurospheres of similar diameter were used in this assay.

P19 Embryonal Carcinoma Cell Culture and Neural Differentiation—P19 mouse embryonic carcinoma cells were grown and differentiated as described previously (19, 21). In brief, for the induction of neural differentiation, 1 μM all-*trans*-retinoic acid was added to 5×10^5 cells/ml, kept in suspension to form embryoid bodies (DMEM supplemented with 2 mM glutamine, 2 mM sodium pyruvate, 2.4 μg/ml of sodium bicarbonate, 5 μg/ml of insulin, 30 μg/ml of human apo-transferrin, 100 mM ethanolamine, 30 nM sodium selenite, 100 IU/ml of penicillin, 100 mg/ml of streptomycin, and 10 mM HEPES, pH 7.4). After 2 days of treatment, embryoid bodies were transferred to culture flasks, and the medium was replaced with DMEM supplemented with 10% FBS to allow cell adhesion. After another 2 days, the medium was replaced by defined medium and maintained until the end of differentiation (day 8).

Human iPS Cell Formation and Neural Differentiation—The human-induced pluripotent stem (iPS) cell lineage was obtained and characterized as described previously (22). Human fibroblasts were generated from dermal biopsies of healthy individuals following informed consent under protocols approved by the University of California, San Diego. Briefly, fibroblasts were infected with retrovirus containing *OCT4*, c-*MYC*, *KLF4*, and *SOX2* human cDNAs (23). After 2 days, fibroblasts were plated on mitotically inactivated mouse embryonic fibroblasts (Millipore) with human embryonic stem cell medium. Following formation of iPS cell colonies, they were directly transferred into Matrigel-coated dishes (BD) containing mTeSR1 (StemCell Technologies). After embryoid body formation in low-adherence dishes in the absence of FGF-2, cell aggregates were allowed to attach to polyornithine-

and laminin-coated dishes in DMEM/F-12 (Life Technologies) supplemented with 1% N2 (Life Technologies). Following rosette visualization, they were dissociated with accutase (Millipore) and plated into coated dishes with NPC medium (DMEM/F-12 supplemented with 0.5% N2; 1% B-27 and FGF-2) to achieve a homogeneous population of NPC. Neural differentiation was induced with 1 μM retinoic acid in NPC medium in the absence of FGF-2 for 3 weeks. Mature embryoid bodies were dissociated and plated in polyornithine- and laminin-coated dishes in NPC media without FGF-2.

Immunocytochemistry—Immunofluorescence procedures have been described in detail elsewhere (24, 25). Plated neurospheres were fixed in 4% paraformaldehyde (PFA) for 20 min and then blocked/permeabilized in 3% FBS, 0.1% Triton X-100 in PBS for 30 min. After 2 h of incubation with primary antibodies against β3-tubulin (Sigma), MAP-2 (Cell Signaling), S100β (Calbiochem), nestin (Millipore), GFAP (DAKO) at 1:500 dilutions, and against B2BkR (1:1000, BD) in PBS with 3% FBS, 0.1% Triton X-100, NPCs were washed, and anti-mouse Alexa 555-conjugated and anti-rabbit Alexa 488-conjugated secondary antibodies (Life Technologies) at 1:500 dilutions were added. After washing with PBS, DAPI solution (Sigma; 0.3 μg/ml) was used as a nuclear stain. Coverslips were mounted, and slides were analyzed under a fluorescence microscope (Axiovert 200, Zeiss).

BrdU Incorporation Assay—Cell proliferation was measured following incubation with 0.2 μM 5-bromo-2-deoxyuridine (BrdU; Sigma) for 14 h. Antigen retrieval was performed following fixation of cells with 4% PFA. Cells were incubated for 30 min in 1.5 M HCl, washed in PBS, and incubated for 2 h with rat anti-BrdU (1:500, Abcam). Alexa 488-conjugated secondary antibodies were used at 1:500 dilutions. After washing with PBS, DAPI solution (0.3 μg/ml) was used as a nuclear stain. Slides were mounted and analyzed by fluorescence microscopy. In this assay, only migrated cells were considered for analysis. The percentages of BrdU-positive cells were calculated as the ratio of immunolabeled cells over the total number of DAPI-stained cells.

Western Blot Analysis—In vitro neural-differentiated cells obtained from different sources or cells from cortical primary cultures were washed once with PBS then incubated in RIPA lysis buffer (50 mM Tris-HCl, pH 7.4, 150 mM NaCl, 1 mM EDTA, 0.5% sodium deoxycholate, 0.1% Nonidet P-40 supplemented with protease inhibitors mixture (Amresco)). Cells were harvested and homogenized on ice. The lysates were then centrifuged for 10 min at 14,000 $\times$ *g*. The concentration of soluble protein in the supernatant was determined by using the Bradford reagent. For Western blot analysis, 10 μg of soluble protein extracts were separated in a 10% SDS-PAGE, transferred to nitrocellulose membranes, and immunoblotted using antibodies against β3-tubulin (1:1000, Sigma), GFAP (1:1000, DAKO), tyrosine hydroxylase (1:1000, Millipore), 5-hydroxytryptamine (1:1000, Abcam), GAD65 (glutamic acid decarboxylase, 1:1000, Millipore), and β-actin (1:2000, Sigma). Horseradish peroxidase-conjugated secondary antibodies were added (1:2000, Jackson ImmunoResearch), and antibody binding was detected by using the enhanced chemiluminescence Luminol reagent (Santa Cruz). Autoradiography films were exposed to the membranes and developed using a Kodak film processor. Band intensities were determined by densitometry and reported as ratios of neuronal and glial markers over β-actin contents. Densitometry analysis was performed using ImageJ software (NIH). Background values were subtracted from all densitometric determinations.

Flow Cytometry Analysis—Flow cytometry procedures were in agreement with previously published protocols (24, 26). Neurospheres and cortical primary cultures were centrifuged for 5 min at 200 $\times$ *g* and dissociated to a single cell suspension. Cells were fixed for 20 min in ice-cold 1% PFA in PBS, washed with PBS supplemented with 2% FBS, and incubated for 2 h with primary antibodies specific for neural markers (β3-tubulin, GFAP, nestin, and neuronal specific enolase (NSE, BioMeda, Foster City, CA)) at 1:500 dilutions. Following a washing step with PBS, cells were incubated with 1:500 Alexa 488- or 555-conjugated secondary antibodies (Life Technologies) and then analyzed on a flow cytometer (Fc500, Beckman Coulter, Fullerton, CA). An argon laser line was used for fluorescence excitation (FL1 525 nm and FL2 575 nm, band pass filter). Fifty-thousand events were acquired per sample with fluorescence measured in logarithmic scales. Background fluorescence was measured using unlabeled cells and cells labeled with secondary antibody alone and used to set gating parameters between positive and negative cell populations. Forward and side light-scatter gates were used to exclude cell aggregates and small debris.

Data were analyzed using the Cyflogic software and plotted in a histogram format. All histograms were smoothed by the software. Fluorescence gates were set below 2% of blank histogram and events corresponding to a fluorescence signal exceeding this percentage were considered as positive events. The results are reported as mean $\pm$ S.D. of positively stained cells.

TUNEL Assay—The effect of HOE-140 treatment on NPC viability was determined using the In Situ Cell Death Detection Kit (Roche Applied Science), according to the protocol provided by the manufacturer. For the negative control, instead of being incubated with the TUNEL reaction mixture, cells were kept in the absence of terminal transferase. For the positive control, cells were incubated with DNase I (3 units/ml, Ambion) for 10 min at room temperature. Thirty-thousand events were acquired in a flow cytometer (Beckman Coulter, Fc500) and analyzed with the Cyflogic software.

Reverse Transcription and Quantitative Polymerase Chain Reaction—Total neurosphere RNA was extracted using the TRIzol reagent (Life Technologies). Following DNase I treatment, 3 μg of RNA was reverse transcribed into cDNA using SuperScript II Reverse Transcriptase (Life Technologies). Quantitative SYBR Green real-time PCR was performed with the Step One Plus Instrument (Life Technologies). Each 25 μl of SYBR Green reaction consisted of 25 ng of cDNA, 12.5 μl of 2$\times$ SYBR Green Universal PCR Master Mix (Life Technologies), and 200 nM of each forward and reverse primers. Unless otherwise stated, primer sequences were designed using Primer Express Software and can be found in Table 1. Real-time PCR were performed using the temperature protocol 50 °C for 2 min, 95 °C for 10 min, and 50 cycles of 95 °C for 15 s and 60 °C for 1 min, followed by a dissociation curve protocol for evalua-

TABLE 1
Primer sequences and amplicon sizes (base pairs, bp) of cDNAs coding for neurotransmitter receptors, nitric oxide-related enzymes, neural markers, transcription factors, and GAPDH used for real-time PCR

Gene	Forward primer (5′-3′)	Reverse primer (5′-3′)	bp	Ref.
P2X1	GAGAGTCGGGCCAGGACTTC	GCGAATCCCAAACACCTTGA	233	66
P2X2	TCCCTCCCCCACCTAGTCAC	CACCACCTGCTCAGTCAGAGC	149	66
P2X3	CTGCCTAACCTCACCGACAAG	AATACCCAGAACGCCACCC	150	66
P2X4	CCCTTTGCCTGCCCAGATAT	CCGTACGCCTTGGTGAGTGT	145	66
P2X5	GGATGCCAATGTTGAGGTTGA	TCCTGACGAACCCTCTCCAGT	81	66
P2X6	CCCAGAGCATCCTTCTGTTCC	GGCACCAGCTCCAGATCTCA	152	66
P2X7	GCACGAATTATGGCACCGTC	CCCCACCCTCTGTGACATTCT	171	66
P2Y1	AACCGTGATGTGACCACTGA	TTCAACTTGTCCGTTCCACA	216	67
P2Y2	TGCTGGGTCTGCTTTTTGCT	ATCGGAAGGAGTAATAGA	209	67
P2Y4	TCGATTTGCAAGCCTTCTCT	CCATAGGAGACCAGGGTGAT	215	67
P2Y6	TGCTGCTACCCCCAGTTTAC	TGGCATAGAAGAGGAAGCGT	246	67
P2Y12	CTGTTTTTTGCTGGGCTCATC	GCGGATCTGGAAGAAAATCCT	60	
P2Y13	GGATGCAGGGCTTCAACAA	GCAGCTGTGTCATCCGAGTGT	60	
P2Y14	GGTGGGTTTCGCCTCATGT	CCTCAGGTGACCGGCATCT	56	
M1 mAChR	CTGTCACGGTCATGTGTACACTGT	CCGGGCTCGGTTTTCTGT	62	
M2 mAChR	CAAAAATGGCAGGCATGATG	GGCCCAGAGGATGAAGGAAA	59	
M3 mAChR	CGACGTGGTGTGATGATTGG	ATGGCAGGAGCCCATAGGA	62	
M4 mAChR	CACCAAACCCCTCACCTATCC	CGATCATGAGACCTGCCATCT	59	
M5 mAChR	CCATAATCCTGTCCGAATGGA	ATCCCGTGGCATTAGTTAGCA	64	
eNOS	GACTTTTAAGGAAGTAGCCAATGCA	CCATACAGGATAAGTCGCCTTCAC	93	
nNOS	CCAATGTTCACAAAAAACGAGTCT	TCGGCTGGACTTAGGGCTTT	77	
Argininosuccinate synthetase	TGCACTCTATGAGGACCGCTATC	AGGCCTGGCGAGAGAGGTGCCTAG	49	
B1BkR	CCAGGGTTCGTCATCACTATCTG	GCAAAAGGAAGAAGGACAAGACTAA	73	68
B2BkR	CCCTTCCTCTGGGTCCTCTT	CAGAACACGCTGAGGACAAAGA	65	68
β3-Tubulin	GAGACCTACTGCATCGACAATGAAG	GCTCATGGTAGCAGACACAAGG	111	25
GFAP	AAGAGTGGTATCGGTCCAAGTTTG	CAGTTGGCGGCGATAGTCAT	107	25
S100β	TGGTTGCCCTCATTGATGTCT	CCCATCCCCATCTTCGTCC	179	
GAPDH	TGCACCACCAACTGCTTAG	GGATGCAGGGATGATGTTC	117	66
Ngn1	CAGTAGTCCCTCGGCTTCAG	AAGCAGGGTGTCGTATGGAG	102	69
Notch1	CACCACGCCTCTCCCACCTGCCTGTAGC	TGCCTGTGTGCTTAGTGTGCCCGGAGTC	209	70
Stat3	TATCTTGGCCCTTTGGAATG	GTGGGGATACCAGGATGTTG	284	71
NeuroD1	CTTCCCGGTGCATCCCTACTCCTACC	AGGAAGGGCTGGTGCAATCAGTTAGG	167	70

tion of the specificity of the amplicon produced in each reaction. A distinct peak indicated that a single DNA sequence was amplified during PCR.

Standard curves were measured for each primer set and cDNA sample to verify the efficiency of the reaction. As the efficiency of all reactions was >95%, the $2^{-\Delta\Delta Ct}$ parameter was used for relative quantification of gene expression. The data shown were obtained from three independent samples and RT-PCR real-time reactions were prepared in triplicates for each analyzed gene. *Glyceraldehyde-3-phosphate dehydrogenase* (*GAPDH*) gene expression was determined as endogenous control.

Calcium Imaging by Confocal Microscopy—Intracellular calcium transients were measured by fluorescence imaging of differentiated cells using the calcium indicator dye fluo-3 AM as described elsewhere (19). Differentiated neurospheres were loaded with 5 μM fluo-3 AM in 0.5% DMSO and 0.1% of F-127 pluronic acid for 1 h at 37 °C. After three washes with culture medium, cells were placed in a warm chamber and fluorescence emissions were captured by a LSM 510-Meta confocal microscope (Zeiss). Following chronic treatment with HOE-140, the inhibitor was removed from the cell culture 1 h prior to calcium measurements by medium change and washing the cell layers five times. Fluo-3 AM was excited using the 488 nm line of argon ion laser, and the emitted light was detected at 515–530 nm using a band-pass filter. Time kinetics of free intracellular calcium ($[Ca^{2+}]_i$) variations were constructed from over 300 images collected in 1-s intervals. The fluorescence intensities (F) were calibrated in a solution containing 5 mM ionophore (F_{max}) and 10 mM EGTA (F_{min}) to provide an estimation of the absolute change in the intracellular calcium concentration using the following equation: $[Ca^{2+}]_i = K_d[(F - F_{min})/(F_{max} - F)]$; assuming a 450 nM K_d for fluo-3 AM. $[Ca^{2+}]_i$ levels of cell populations prior and following stimulation were calculated using the average value of at least five fields of observation in independent experiments.

Whole Mount in Situ Hybridization—Whole mount *in situ* hybridizations were adapted from a protocol described elsewhere (27). In summary, mouse embryos were fixed in 4% PFA, treated with proteinase K, re-fixed with 4% PFA, 0.1% glutaraldehyde and hybridized overnight with 1 μg of digoxigenin-labeled RNA sense and antisense probes. After the wash, embryos were treated with a solution containing 10% goat serum, 1% Boehringer Block, and 0.1% Tween 20 in PBS at 4 °C for 2 h and then incubated overnight with anti-digoxigenin alkaline phosphatase antibodies at 4 °C. Finally, the embryos were washed in 0.1% BSA and stained overnight with alkaline phosphatase substrate at 4 °C. *B2BkR* sense (5′-GGACTCCCTACAACACAGAAC-3′) and antisense (5′-GGACAAAGAGGTTCTCCAGTG-3′) probes were generated by linearization and *in vitro* transcription of pBluescript II KS-*B2BkR* (NM_009747.2) with XbaI/T3 and XhoI/T7, respectively.

Statistical Analyses—The results were expressed as mean ± S.D. from three or more independent experiments, unless otherwise stated. Statistical comparisons between different treatments were done by either a Student's t test or one-way analysis of variance by using GraphPad Prism 5.1 software (Graph-Pad Software Inc.). For quantification of immunolabeled $BrdU^+$ cells, a minimum of 300 and up to 800 cells per sample was analyzed using ImageJ software. For

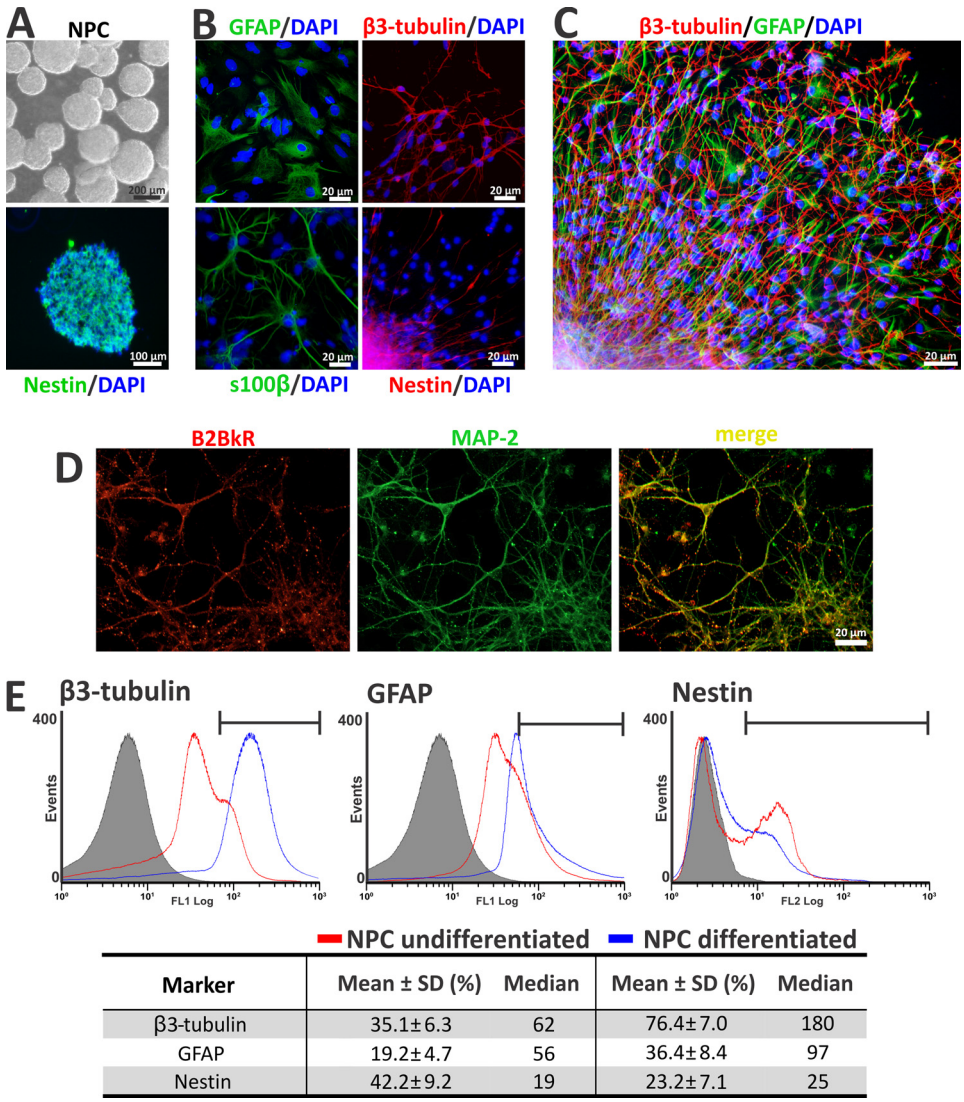

Marker	Mean ± SD (%)	Median	Mean ± SD (%)	Median
β3-tubulin	35.1±6.3	62	76.4±7.0	180
GFAP	19.2±4.7	56	36.4±8.4	97
Nestin	42.2±9.2	19	23.2±7.1	25

FIGURE 1. ***In vitro* neural progenitor differentiation.** *A,* neural progenitor was obtained from rat embryo telencephalon (E14) induced for 7 days to proliferation for formation of neurospheres. *Upper panel*, phase-contrast image of primary undifferentiated neurosphere (NPC). *Lower panel*, nestin is highly expressed in undifferentiated neurospheres. *B,* typical immunofluorescence images of neurospheres on day 7 of differentiation. Differentiated neurospheres express specific protein markers for progenitor cells (nestin), astrocytes (GFAP and s100*β*), and neurons (*β3-tubulin*). *C*, radial cell migration pattern and neural maturation. The radial migration observed near the neurospheres consists mainly of precursor cells and astrocytes, whereas neuronal migration occurs to form a distal network. *D*, detection of co-expression of B2BkR and MAP-2, indicating that B2BkR are expressed in mature neurons. *E*, flow cytometry analysis of neural markers expression of undifferentiated (*red lines*) and differentiated (*blue lines*) neurospheres. Events with higher fluorescence as those in the control histograms (within the area delimited by *bars*) were considered positive and quantified in the table below. The data shown are representative of at least three independent experiments.

flow cytometry, a minimum of 30,000 cells was analyzed per sample. The criteria for statistical significance were set at $p < 0.05$.

RESULTS

B2BkR and Neural-specific Protein Expression Profile during Neurosphere Differentiation—Rat telencephalon cells were cultured in growth medium to allow neural stem cells and NPCs to proliferate and form neurospheres (Fig. 1*A*). Consistent with Martins *et al.* (24), undifferentiated neurospheres expressed high levels of GFAP and nestin, in some cases co-expressed in the same cell. Following induction of differentiation, the number of nestin-positive cells in the outer layers of migrating cells decreased, whereas cells within the neurosphere remained undifferentiated (24). Neuron-specific protein *β*3-tubulin, and astrocyte-specific s100*β* were expressed at high levels in differentiated cells (Fig. 1*B*). Cells elongated in a radial pattern with intense staining for GFAP and nestin. Network-forming differentiated cells were located most distally (Fig. 1*C*). Double-immunostaining against MAP-2 and B2BkR on day 7 of differentiation revealed that the B2BkR was expressed by mature neurons, as shown in Fig. 1*D*.

Analysis by flow cytometry clearly confirmed the difference in the expression of proteins specific for un- or differentiated neurospheres (Fig. 1*E*). Expression of the neuronal marker *β*3-tubulin was detected in 35 and 76% of undifferentiated and differentiated cells, respectively. GFAP and nestin were present in 19 and 42% of undifferentiated cells, respectively. In differentiated cells, the expression of GFAP increased to 36%, and nestin expression was reduced to 23% of the cell population.

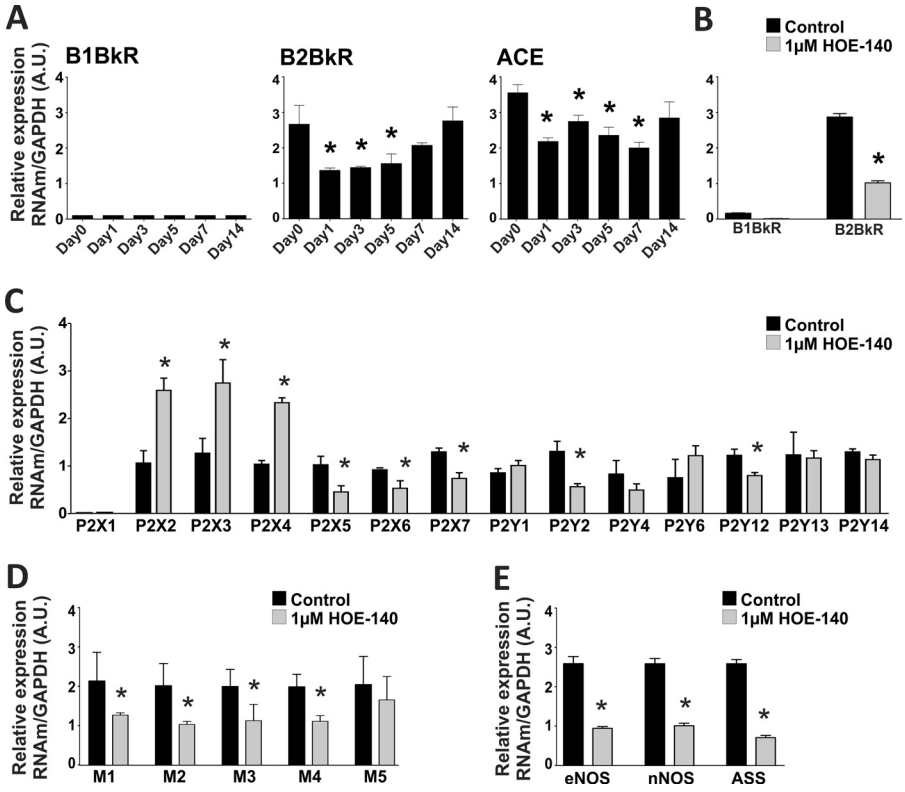

FIGURE 2. **Gene expression of components of the kallikrein-kinin system and neurotransmitter receptors after chronic treatment with 1 μM HOE-140 along rat neural differentiation.** *A*, *B1BkR* gene expression could not be detected during 14 days of neurosphere differentiation, whereas *B2BkR* and angiotensin-converting enzyme (*ACE*) expression showed an initial reduction after differentiation induction. *B2BkR* expression increased again during the final differentiation. *B*, *B2BkR* gene expression after NPC treatment with HOE-140 during 7 days. *C*, specific B2BkR inhibition for 7 days caused an alteration in ionotropic and metabotropic purinergic receptor gene expression. *D* and *E*, chronic HOE-140 treatment led to reduced muscarinic receptor gene expression as well as key proteins involved in nitric oxide formation (neuronal nitric-oxide synthase, nNOS; endothelial nitric-oxide synthase, eNOS; argininosuccinate synthetase, ASS). The data are representative for three independent experiments conducted in triplicate and shown as mean ± S.D. (*, $p < 0.05$).

Throughout differentiation, percentages of neuronal and glial phenotypes increased in the cell population, whereas percentages of NPCs decreased.

B2BkR Inhibition during Differentiation Alters Expression and Activity of Neurotransmitter Receptors—A large number of membrane receptors are expressed to initiate complex sets of sequential transcriptional events important for cell fate determination. The expression of kinin, purinergic, and muscarinic receptors during rat differentiation was quantitatively evaluated by real-time PCR. The expression of the *B1BkR* was lower than the detection limits of the methodology employed, whereas *B2BkR* expression decreased initially and increased during later differentiation. The transcriptional levels of angiotensin-converting enzyme (*ACE*) mRNA controlling lifetime of biologically active kinins remained stable (Fig. 2*A*). Chronic treatment of differentiating rat neurospheres with HOE-140, a specific antagonist of the B2BkR, significantly decreased the gene expression of *B2BkR* (Fig. 2*B*). The expression of other components of the kallikrein-kinin system in neurospheres and Bk release were already reported in a previous publication of our group (24). Quantitative real-time PCR analysis revealed a significant increased expression of rat *purinergic P2X2*, *P2X3*, and *P2X4* receptor subunits and decreased expression of *P2X5*, *P2X6*, *P2X7*, *P2Y2*, and *P2Y12* subtypes (Fig. 2*C*). The expression of *M1–M4 muscarinic receptors* decreased following chronic treatment with HOE-140, corroborating previous data obtained from P19 cells (19) and supporting the existence of an interrelationship between cholinergic and kallikrein-kinin systems (Fig. 2*D*). Thus, Bk influences the expression of purinergic and cholinergic receptors during neural differentiation. We also investigated the presence of transcripts of *endothelial* and *neuronal nitric-oxide synthase* (*eNOS* and *nNOS*) and *argininosuccinate synthetase* (*ASS*) along neural differentiation. Considering the role of NO in neural differentiation and proliferation (28–30), the inhibitory effects of HOE-140 on gene expression of *eNOS, nNOS*, and *ASS* further indicate functions for the B2BkR during neural differentiation (Fig. 2*E*).

HOE-140-induced effects on iono- and metabotropic receptors in differentiated rat neurospheres were also studied by using calcium imaging. HOE-140 was completely removed from the cells following several washes 1 h before the beginning of the experiment. ATP- and UTP-induced receptor responses diminished in the presence of HOE-140, reflected by changes in $[Ca^{2+}]_i$ peak values from Δ1695 ± 190 to Δ1044 ± 279 nM ($p = 0.0371$) and from Δ1320 ± 126 to Δ703 ± 189 nM ($p = 0.0055$), respectively (Fig. 3). Effects of chronic B2BkR blockade on muscarinic receptor activity were even more evident. Muscarine-induced $[Ca^{2+}]_i$ transients with peak values of Δ2023 ± 304 nM were reduced to Δ243 ± 205 nM ($p = 0.0016$) when HOE-140 was present during the course of differentiation. B2BkR activity was also reduced by 37% following chronic blockade of

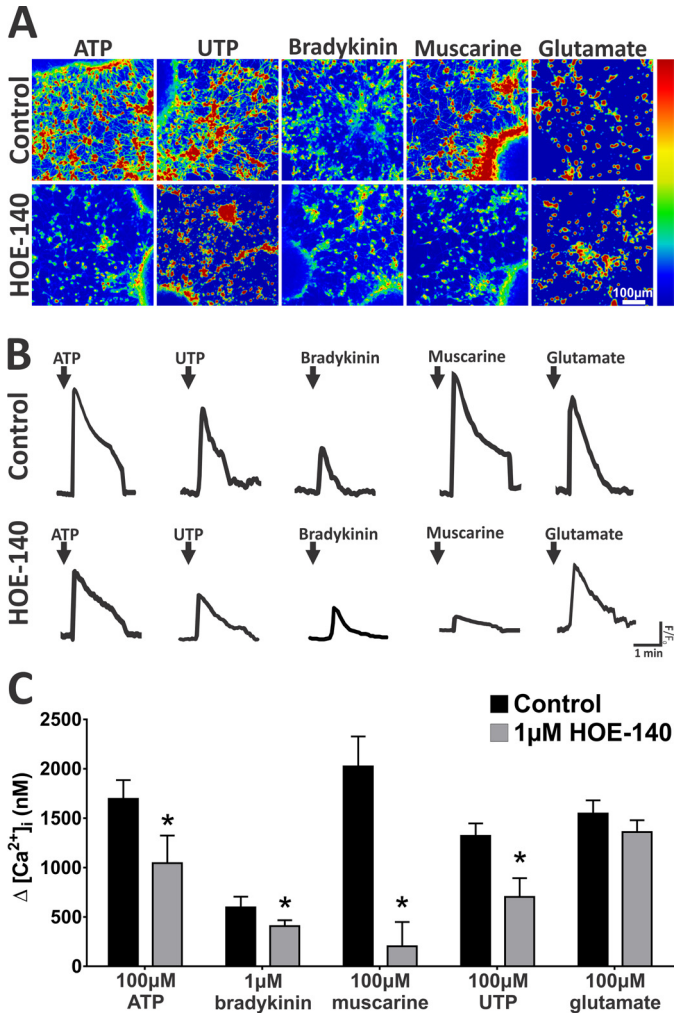

FIGURE 3. **Effects of chronic B2BkR blockade on neurotransmitter-induced $[Ca^{2+}]_i$ transients in differentiated rat neurospheres.** *A*, representative images following stimulation by 100 μM ATP, 100 μM UTP, 1 μM Bk, 100 μM muscarine, or 100 μM glutamate in cells differentiated for 7 days in the absence or presence of 1 μM HOE-140. HOE-140 was removed from cell cultures by medium change and washing the cell layers five times 1 h before staining cells with fluo-3 AM. $[Ca^{2+}]_i$ levels were monitored using calcium imaging by confocal microscopy, calculated using the average value of at least five fields of observation and represented in a color gradient. *B*, kinetics of $[Ca^{2+}]_i$ transients. *Arrows* indicate the time point of agonist application (F_o values represent basal $[Ca^{2+}]_i$ levels of nonstimulated cells). *C*, mean values of $[Ca^{2+}]_i$ peak amplitudes in differentiated neurospheres pre-treated or not with 1 μM HOE-140 were calculated as described under "Experimental Procedures" and shown as mean ± S.D. ($n = 3$) (*, $p < 0.05$ by Student's *t* test. ATP, $p = 0.0371$; Bk, $p = 0.0058$; muscarine, $p = 0.0016$; UTP, $p = 0.0055$; glutamate, $p = 0.1688$).

kinin-B2 receptors followed by wash-out of the antagonist prior to calcium measurements (control = Δ596 ± 109 nM; treated with HOE-140 = Δ407 ± 59 nM) ($p = 0.0058$). The observed changes did not affect all signaling systems as no significant changes in glutamate-induced $[Ca^{2+}]_i$ peak values were observed in cells treated with HOE-140 ($p = 0.1688$).

Effects of Bradykinin and HOE-140 on Cell Death and Proliferation—We evaluated the effects of B2BkR activation and inhibition on cellular proliferation and whether HOE-140 treatment would induce cell death or have any visible effects on cellular morphology and cell viability. To this end, rat neurospheres were differentiated for 7 days in the absence or presence of 1 μM HOE-140 (Fig. 4) and analyzed by TUNEL staining. Flow cytometry analysis revealed that the chronic treatment with 1 μM HOE-140 did not affect the number of $TUNEL^+$ cells when compared with control experiments (5.1 ± 0.3% $TUNEL^+$ cells) (Fig. 4*A*). The effect of B2BkR blockade on cell proliferation was analyzed by the BrdU incorporation assay (Fig. 4*B*). Approximately 11% of the cells on day 7 of differentiation were proliferative. Similar values were obtained in cells co-treated with 1 μM HOE-140 and 1 μM Bk (9.8 ± 1.3%) or treated with HOE-140 alone (12.5 ± 1.7%). However, in the presence of Bk, cell proliferation was inhibited by ~40% (5.4 ± 2.7% of the cell population; $p = 0.0187$).

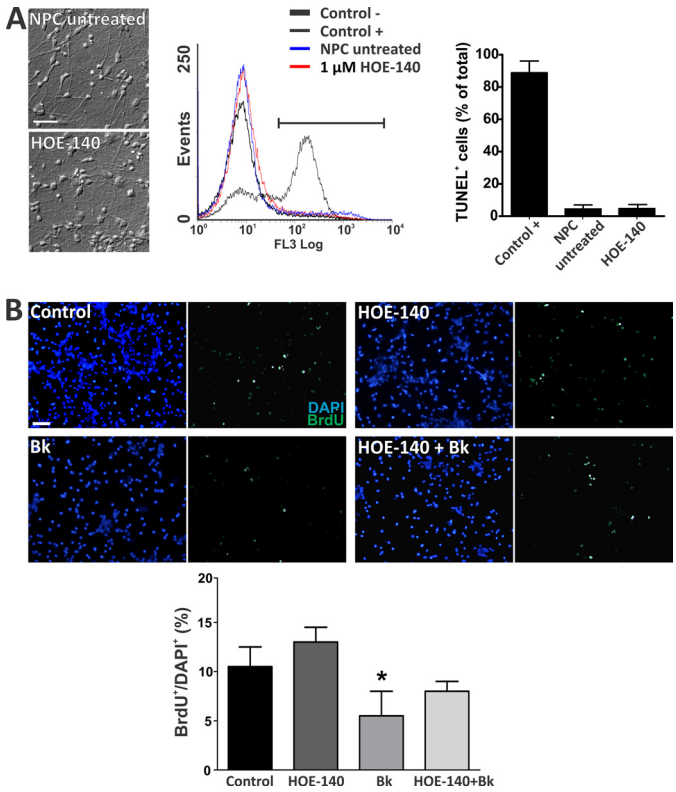

FIGURE 4. **Effects of B2BkR inhibition on rat neural progenitor cell death and proliferation.** *A*, the images show the cellular morphology of rat NPCs differentiated for 7 days in the presence or absence of 1 μM HOE-140. Percentages of cells on day 7 of differentiation undergoing cell death were determined by flow cytometry using the TUNEL assay. For negative control, we used only the marker reagent. For the positive control, NPCs were treated with DNase I to induce DNA strand breaks and verify their positive staining. Thirty-thousand events were acquired in a flow cytometer (Beckman Coulter, Fc500) and analyzed with the Cyflogic software. Cell death measured by the TUNEL assay was not significantly altered in the presence of 1 μM HOE-140 ($n = 2$). *Scale bars* = 20 μm. *B*, immunodetection of BrdU (0.2 μM) after a 14-h pulse in differentiated neurospheres in the presence of 1 μM Bk in the absence or presence of 1 μM HOE-140. BrdU incorporating nuclei are shown in *green*. The graph shows the quantification of proliferation in different treatments as the ratio of $BrdU^+$ over $DAPI^+$ cells. The percentage of proliferating $BrdU^+$ cells is significantly lower in NPCs treated with bradykinin. Six fields were evaluated for each treatment (*, $p < 0.05$). *Scale* = 50 μm.

Bradykinin Favors Neurogenesis in Distinct Cell Models—The progress of neural differentiation is closely related to cell migration and neuron-glia interactions (31–33). In this process, different factors act on neural progenitor cells for defining their fate. Thus, we studied whether the effects of B2BkR activation or blockade would influence migration prior to neuronal and glial maturation. Seven days after rat neurospheres were plated onto adherent surfaces in medium deprived of growth factors;

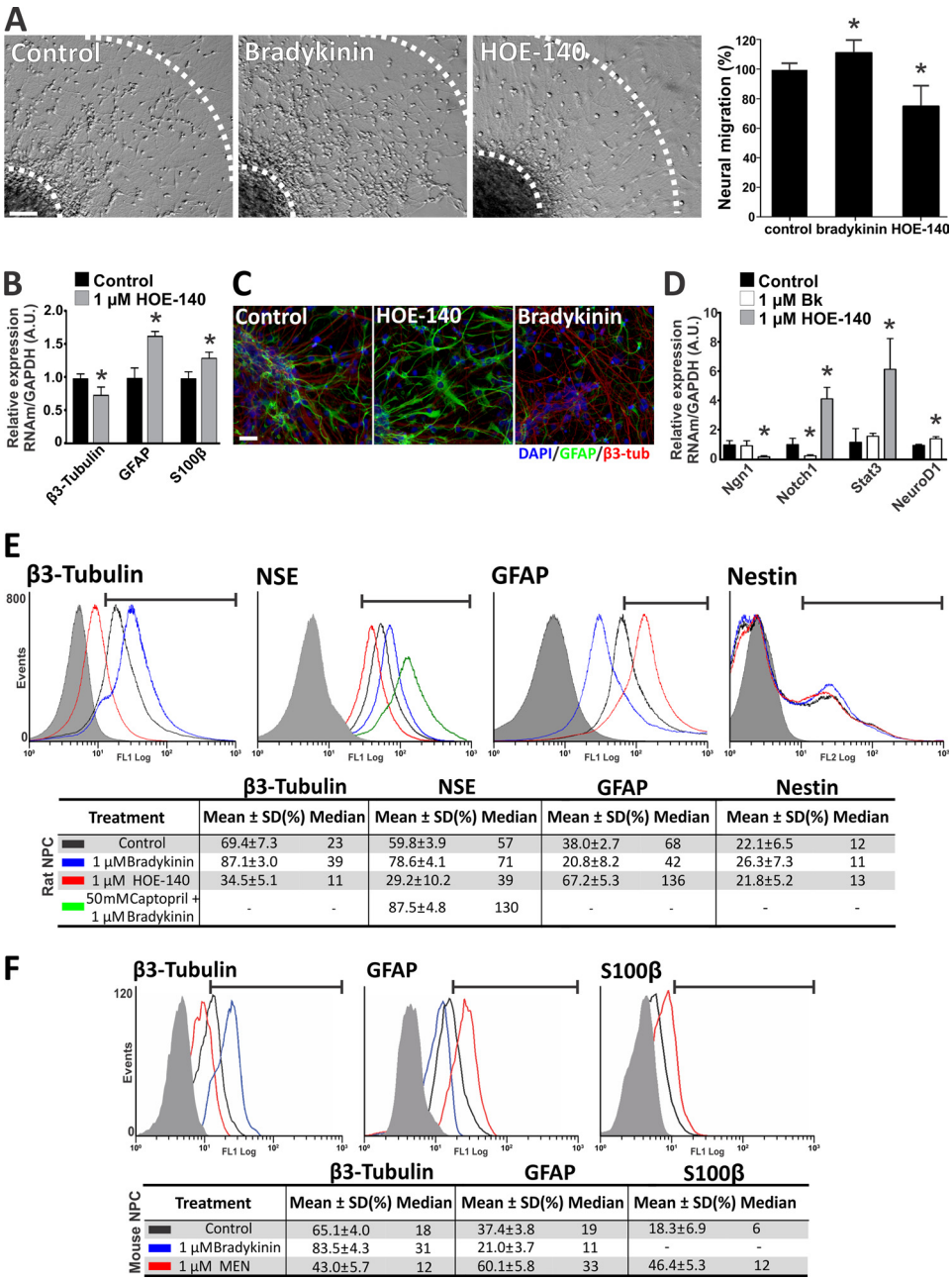

	Treatment	β3-Tubulin Mean ± SD(%)	β3-Tubulin Median	NSE Mean ± SD(%)	NSE Median	GFAP Mean ± SD(%)	GFAP Median	Nestin Mean ± SD(%)	Nestin Median
Rat NPC	Control	69.4±7.3	23	59.8±3.9	57	38.0±2.7	68	22.1±6.5	12
	1 μM Bradykinin	87.1±3.0	39	78.6±4.1	71	20.8±8.2	42	26.3±7.3	11
	1 μM HOE-140	34.5±5.1	11	29.2±10.2	39	67.2±5.3	136	21.8±5.2	13
	50 mM Captopril + 1 μM Bradykinin	-	-	87.5±4.8	130	-	-	-	-

	Treatment	β3-Tubulin Mean ± SD(%)	β3-Tubulin Median	GFAP Mean ± SD(%)	GFAP Median	S100β Mean ± SD(%)	S100β Median
Mouse NPC	Control	65.1±4.0	18	37.4±3.8	19	18.3±6.9	6
	1 μM Bradykinin	83.5±4.3	31	21.0±3.7	11	-	-
	1 μM MEN	43.0±5.7	12	60.1±5.8	33	46.4±5.3	12

FIGURE 5. **Bradykinin enhances neurogenesis, whereas HOE-140 promotes gliogenesis in neurosphere differentiation.** *A*, phase-contrast images representing radial migration pattern after 7 days of neural differentiation in the presence of 1 μM bradykinin (Bk) or 1 μM HOE-140. The region enclosed *between the dotted lines* comprises ~95% of migrated cells. Scale = 100 μm. *B*, neural markers gene expression was changed upon B2BkR inhibition. Note that the GFAP and S100β expression levels were increased, whereas β3-tubulin expression was decreased. The data are representative of three independent experiments conducted in triplicate and show as mean ± S.D. ($n = 4$) (*, $p < 0.05$). *C*, immunostaining of rat neurospheres differentiated in the presence of 1 μM Bk or 1 μM HOE-140. *Scale*, 20 μm. *D*, transcription factor and neural marker gene expression was changed upon B2BkR inhibition or activation. The data are representative of three independent experiments conducted in triplicate and shown as mean ± S.D. (*, $p < 0.05$ by Student's *t* test compared with control data. *Ngn1* (*neurogenin 1*), Bk, $p = 0.8304$; HOE-140, $p = 0.0098$; *notch 1*, Bk, $p = 0.0139$; HOE-140 $p = 0.0038$; *Stat3*, Bk, $p = 0.0178$; HOE-140, $p = 0.0008$; *NeuroD1*, Bk, $p = 0.0302$). *E*, flow cytometry analysis of GFAP, β3-tubulin, neuronal specific enolase (*NSE*), and nestin expression in rat neurospheres differentiated for 7 days in the presence of Bk, HOE-140 or captopril, and Bk. Representative histograms compare expression levels of neural markers in differentiated rat neurospheres, treated with Bk, HOE-140, and captopril + Bk. *F*, analysis of β3-tubulin, GFAP, and S100β expression in mouse neurospheres differentiated for 7 days in the presence of 1 μM bradykinin or 1 μM MEN-11270 (MEN), a B2BkR antagonist. The data shown are representative of at least two independent experiments. The *blank histograms in gray* reveal fluorescence emission data in the absence of primary antibodies. The data shown are representative of at least five independent experiments.

NPCs presented a radial migration pattern closely linked to a gradient of maturation (Fig. 5). Fig. 5*A* shows representative images of differentiated neurospheres, where the region enclosed *between the dotted lines* comprises ~95% of migrating cells. Cells migrated 15% farther from the edge of neurospheres in the presence of Bk compared with control cultures. Conversely, blockade of B2BkR by HOE-140 treatment resulted in a 25% smaller migration distance despite displaying the same radial pattern. These results suggest that alteration of migration may also influence neurogenesis and gliogenesis.

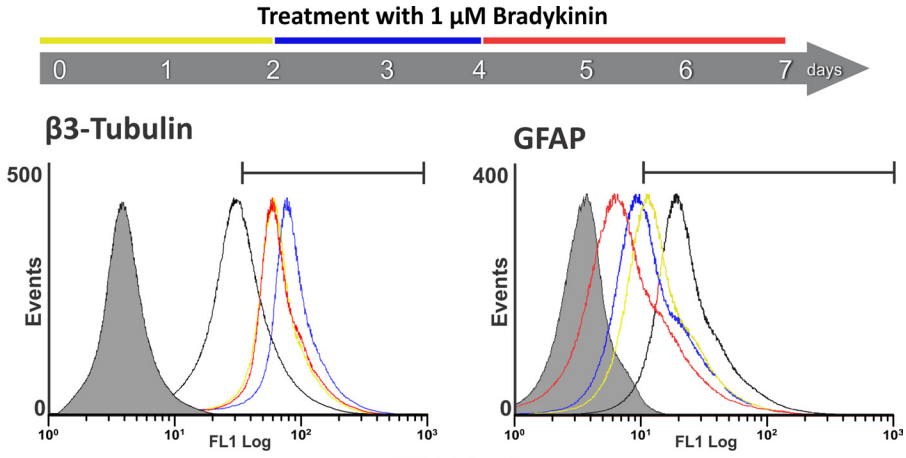

Treatment	β3-Tubulin Mean ± SD (%)	β3-Tubulin Median	GFAP Mean ± SD (%)	GFAP Median
Untreated NPC	65.1 ± 5.3	32	43.6 ± 8.5	25
1μM Bradykinin 0-2	74.6 ± 3.8	58	20.1 ± 3.7	14
1μM Bradykinin 2-4	84.8 ± 5.2	75	17.8 ± 2.8	11
1μM Bradykinin 4-7	75.3 ± 5.7	57	11.3 ± 4.1	6

FIGURE 6. **Role of B2BkR on different days of rat neurospheres differentiation.** Bradykinin was applied between days 0–2, 2–4, and 4–7, and was removed at the end of each period. Representative flow cytometry histograms comparing the expression of neural markers in control differentiated neurospheres (*black*) or at different times of treatment with 1 μM bradykinin (*Bk*), between days 0–2 (*yellow*), 2–4 (*blue*), and 4–7 (*red*). The most significant effects on neural differentiation were observed in intermediate and final phases. The data shown are representative of at least four independent experiments.

Additionally, chronic treatment of NPCs with HOE-140 decreased the expression of *β3-tubulin* by 25 ± 13% (p = 0.0477), whereas *GFAP* and *S100β* expression levels were significantly increased by 65 ± 9 (p = 0.0024) and 31 ± 8% (p = 0.0032), respectively (Fig. 5*B*). These results indicate, for the first time, an important role of the B2BkR in neural fate determination, where inhibition of B2BkR activity favors gliogenesis over neurogenesis. B2BkR-mediated effects were confirmed by microscopic analysis of immunostained cells (Fig. 5*C*). Although gliogenesis was reduced, neurogenesis visualized by β3-tubulin expression was much more evident in neurospheres treated with 1 μM Bk throughout the course of differentiation when compared with neurospheres differentiated in the absence of the Bk or in the presence of HOE-140.

We further investigated the expression of neurogenic and transcription factors genes, such as *ngn1* (*neurogenin 1*), *notch1*, *Stat3* (signal transducer and activator of transcription 3), and *NeuroD1*, in differentiated NPCs in the absence or presence of HOE-140 or Bk. Real-time PCR revealed that the treatment with HOE-140 significantly increased the expression of genes related to gliogenesis (*notch 1* and *Stat3*), whereas in the presence of Bk a significant difference of *NeuroD1* expression was obtained compared with the control group (Fig. 5*D*). Conversely, *Ngn1* expression levels were decreased with HOE-140 treatment and *notch 1* levels diminished after Bk treatment.

Flow cytometry analysis revealed that the expression of the neuronal markers β3-tubulin and NSE following Bk treatment were increased from 69.4 ± 7.3 to 87.1 ± 3.0% and 59.8 ± 3.9 to 78.6 ± 4.1%, respectively (Fig. 5*E*). Co-treatment with captopril and Bk greatly increased the percentage of NSE^+ cells, reaching 87.5 ± 4.8% after ACE inhibition, given by the increased availability of Bk. In contrast, prolonged activation of B2BkR decreased the glial population from 38.0 ± 2.7 to 20.8 ± 8.2%, whereas the population of $nestin^+$ cells did not show any significant variation, remaining at ~22%. Chronic treatment with HOE-140 also altered the phenotypic population features; however, this treatment showed a bias of gliogenesis. The percentage of $GFAP^+$ cells almost doubled from 38.0 ± 2.7 to 67.2 ± 5.3%. Percentages of $nestin^+$ cells did not change significantly under Bk treatment. Similar results were obtained by flow cytometry analysis of mouse NPCs differentiated in the presence of Bk or MEN-11270 (another B2BkR specific inhibitor) (Fig. 5*F*).

Effects of Bk on neural fate determination may depend on the time of application, *i.e.* its action could be more evident at the beginning or end of differentiation, considering other external and internal factors participating in this process. Thus, Bk was added and removed at specific times during differentiation: 0–2, 2–4, or 4–7 days. Quantification of glia and neuronal populations by flow cytometry revealed that most significant favoring of neurogenesis by Bk occurred in intermediate and late days of differentiation (Fig. 6). Although discrete, the expression of β3-tubulin during this period peaked (84.8 ± 5.2%) and was comparable with those obtained by chronic treatment with Bk along the whole course of differentiation. This may be related mainly to the migration of cells from neurospheres, which is enhanced at intermediate and late stages of differentiation. On the other hand, the decreased GFAP expression was most evident when cells were treated with Bk between days 4 and 7 (11.3 ± 4.1%), in agreement with reversal of the proliferation blockade at the end of differentiation in the presence of HOE-140.

Additionally to immunocytochemistry and flow cytometry, we used Western blot analysis to evaluate relative protein con-

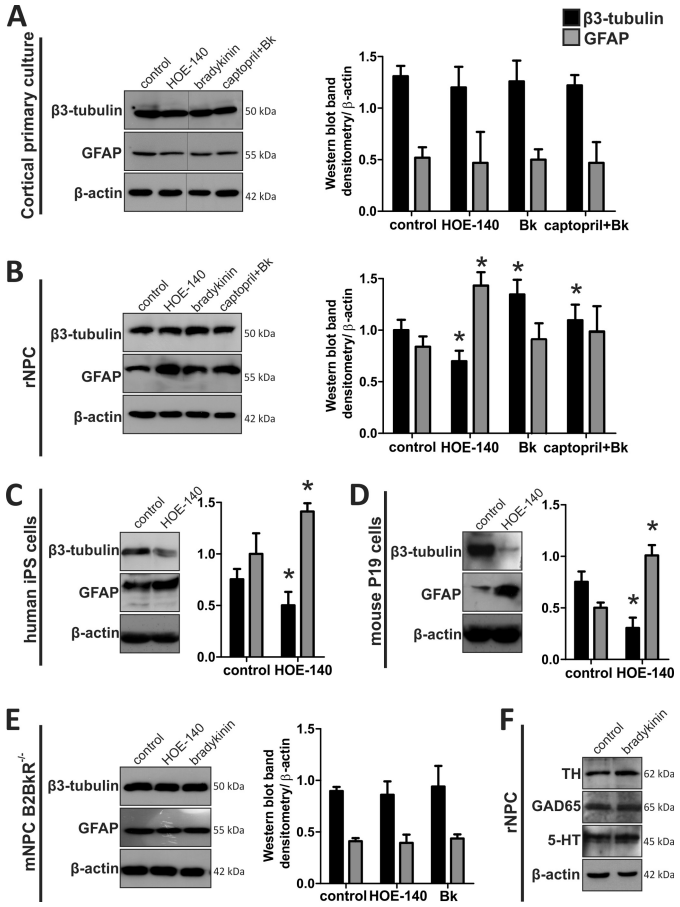

FIGURE 7. **Western blot analysis of neural marker expression.** *A*, immunoblots of protein extracts from newborn rat cortical primary culture after treatment with 1 μM Bk, 1 μM HOE-140, or 50 mM captopril + 1 μM bradykinin. *B*, densitometry of protein extracts from differentiated rat neurospheres ($n = 4$). *C*, densitometry of protein extracts from human-induced pluripotent stem cells ($n = 2$). *D*, densitometry of protein extracts from differentiated mouse P19 carcinoma cells ($n = 3$). *E*, densitometry of protein extracts of differentiated mouse neurospheres obtained from *B2BkR* knock-out mice ($n = 2$). *F*, immunoblots of protein extracts from differentiated rat neurospheres after treatment with 1 μM bradykinin along differentiation (TH, tyrosine hydroxylase; 5-HT, 5-hydroxytryptamine; GAD65, glutamic acid decarboxylase).

tents of β3-tubulin and GFAP in different cell models (Fig. 7). In accordance with the results so far shown, Western blot analysis showed no change in the number of neuronal and glial proteins in primary cortical cultures previously treated with HOE-140 or Bk. We noticed a clear increase in β3-tubulin protein after treatment with Bk or captopril + Bk in rat neurosphere, murine P19, and human iPS cell differentiation. The opposite effect, increased GFAP content, could be observed after differentiation of the same models of rat, mouse, and human cells in the presence of the specific blocker of B2BkR, HOE-140 (Fig. 7, *A–D*). To verify that promotion of neurogenesis resulted from B2BkR activation, neurospheres from the B2BkR knock-out mice were differentiated in the presence of 1 μM Bk or 1 μM HOE-140. After these treatments we found no significant change in neural marker protein content, confirming that neural differentiation was specifically modulated by B2BkR and not by possible side effects of HOE-140 treatment (Fig. 7*E*). The presence of Bk along differentiation did not induce any changes of subpopulation-specific neurotransmitter expression. Immunoblotting against tyrosine hydroxylase (dopaminergic marker), 5-hydroxytryptamine (serotoninergic marker), and GAD65 (GABAergic marker) in neurospheres did not reveal any differences in expression of these markers (Fig. 7*F*).

Neurogenesis Is Favored via B2BkR Only in Differentiating Cells—For confirming specific neurogenic roles of Bk, we investigated whether these effects occurs only in the differentiation process or could also be observed in differentiated neural cells. For this purpose, we used cortical primary cultured cells of newborn rats treated for 7 days without or with 1 μM Bk or 1 μM HOE-140. Flow cytometry analysis of cortical primary cultures pre-treated with Bk or HOE-140 did not reveal any change in percentages of neuronal and glial cells (Fig. 8*A*). Thus, the occurrence of neurons and glia remained constant regardless of treatment, suggesting that the effect of neuronal cell enrichment by Bk via B2BkR occurs only during the process of differentiation.

Considering the influence of the B2BkR in modulating neural differentiation by promoting neurogenesis, we assessed whether this effect would be caused by enzymatic cleavage of Bk with consequent formation of metabolites and activation of the B1BkR. In this context, rat neurospheres were plated and differentiated in the presence of 1 μM Lys-[des-Arg^9]-Bk, an agonist of the B1BkR, or 1 μM R-715, a specific B1BkR antagonist. After this period, we performed flow cytometry analysis to quantify neural marker expression (Fig. 8*B*). There was no change in the number of cells expressing neural markers β3-tubulin and GFAP. Thus, the phenotypic fate determination during neural differentiation does not appear to be influenced by the B1BkR. It is noteworthy that mRNA transcription coding for B1BkR during neural differentiation could not be detected in real-time PCR analysis.

Differentiated Neurospheres Derived from B2BkR$^{-/-}$ Mice Show a Reduction in Neural Migration—Further confirmation of modulation of neurogenesis by Bk and its receptor was obtained in *B2BkR* knock-out mice. The use of *B2BkR*$^{-/-}$ mice to obtain neurospheres allowed further study of the process of cell differentiation and neural migration. To verify the homozygosis in knock-out mice, genomic DNA was extracted from small biopsies of the animals and amplified by PCR with specific primers for *B2BkR* and rate genes. *B2BkR*$^{-/-}$ mice-derived neurospheres revealed the same growth rates of wild-type neurospheres, without visible morphological changes. After plating and induction of neural differentiation of *B2BkR*$^{-/-}$ neurospheres, we observed the same radial pattern, although with decreased migration when compared with control neurospheres from wild-type animals (Fig. 9). The quantification of cell migration between the dotted lines is shown in Fig. 9*A*. In addition, immunocytochemical analysis revealed the same pattern characterized mainly by radial GFAP$^+$ cells and a low migration of β3-tubulin$^+$ cells in *B2BkR*$^{-/-}$ mice neurospheres (Fig. 9*B*). The immunostaining also reveals less β3-tubulin$^+$ cells (~72%) and a high content of GFAP$^+$ cells (47%) in B2BkR$^{-/-}$.

Developmental Expression of B2BkR and Its Effect on Neural Marker Expression during Brain Development—The *B2BkR* is ubiquitously and constitutively expressed in adult healthy tissues. To assess whether it is also expressed in developing mice,

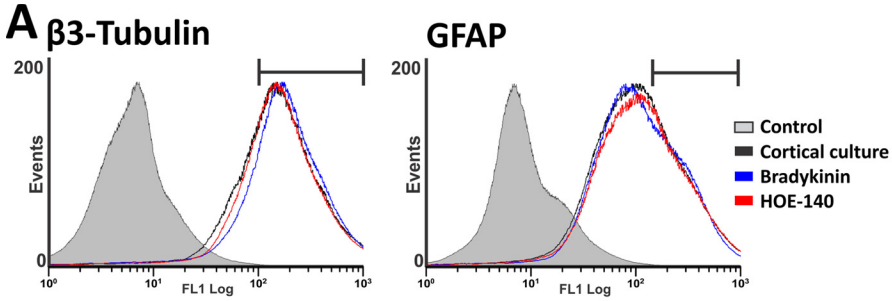

	β3-Tubulin		GFAP	
Treatment	Mean ± SD(%)	Median	Mean ± SD(%)	Median
Control	76.4±9.8	172	38.4±7.5	197
1μM bradykinin	81.2±5.4	198	37.3±2.4	193
1μM HOE-140	78.5±7.3	185	36.8±4.1	202

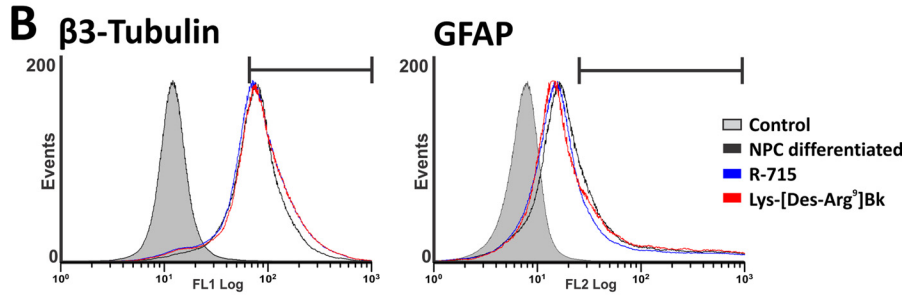

	β3-Tubulin		GFAP	
Treatment	Mean ± SD(%)	Median	Mean ± SD(%)	Median
Control	72.0±4.3	71	31.4±9.5	29
1μM Lys-[Des-Arg^9]-Bk	75.8±8.0	68	36.9±3.2	22
1μM R-715	76.2±6.3	72	34.8±6.1	29

FIGURE 8. **Flow cytometry analysis of β3-tubulin and GFAP expression in cortical primary culture and neurosphere differentiated in the presence of 1 μM Lys-[des-Arg^9]-bradykinin and R-715.** *A*, cortical cells of newborn rats were cultured in the absence or presence of 1 μM bradykinin or 1 μM HOE-140 for 7 days. Representative flow cytometry histograms comparing the expression of neural markers in differentiated neurospheres (*black*), treated with bradykinin (*blue*) or HOE-140 (*red*) ($n = 4$). *B*, representative flow cytometry histograms comparing the expression of neural markers in differentiated neurospheres (*black*), treated with a B1BkR inhibitor, R-715 (*blue*), or a B1BkR agonist, Lys-[des-Arg^9]-bradykinin (*red*) ($n = 3$). The *blank histogram* represents data obtained in the absence of primary antibodies.

expression of *B2BkR* was determined in embryos removed from pregnant dams at various neurogenic developmental time points (E9.5–E12.5) by whole mount *in situ* hybridization with antisense RNA probes (Fig. 10). Mouse *B2BkR* transcripts were detected in neural cells at day E9.5, starting in the optic vesicle (Fig. 10*A*), then increasing their expression pattern to the whole nervous system at days E11.5 (Fig. 10*B*) and E12.5 (Fig. 10*C*). Negative controls with *B2BkR* sense probes did not reveal any specific labeling (Fig. 10*D*). Here, we show for the first time that *B2BkR* is strongly expressed in the developing mouse brain, including telencephalon, diencephalon, and ventral region of midbrain and hindbrain as well as in the spinal cord. For further analysis of the role of B2BkR in developing brains, we verified the expression of *β3-Tubulin* in the telencephalon and cortex at several time points during WT and *B2BkR*$^{-/-}$ mice development (E9.5-adult) (Fig. 10*E*). The developing knock-out mice brains showed significantly less expression of *β3-Tubulin* from E11.5 until adulthood (*, $p < 0.05$; adult, $p = 0.0334$; E9.5, $p = 0.0861$; E11.5, $p = 0.4349$; E14.5, $p = 0.0004$; E17.5, $p = 0.0008$; P0, $p = 0.0001$). Adult *B2BkR*$^{-/-}$ brain express more glial markers, such as *GFAP* (*, $p < 0.05$; adult, $p = 0.0083$) and *S100β* (*, $p < 0.05$; adult, $p = 0.0001$) (Fig. 10*F*). These data indicate that the *B2BkR*$^{-/-}$ brain expresses less neuronal marker and higher levels of glial markers, indicating that Bk-induced actions occur not only during *in vitro* neural differentiation, but are also important for *in vivo* neurogenesis.

DISCUSSION

Bk actions in neurogenesis are suggested based on its participation in determining the cholinergic phenotype of differentiating cells (19), induction of calcium waves (34, 35), neurite formation (36–38), and cell migration. Moreover, Bertram *et al.* (39) demonstrated increased migration of human monocytes induced by Bk. In glioma cells, Lu *et al.* (40) reported augmented migration in the presence of Bk, but this effect was reproduced by B1BkR agonists. In another study, increased migration of chondrosarcoma cells was related to the Bk-activated signaling cascade (41). In summary, Bk or

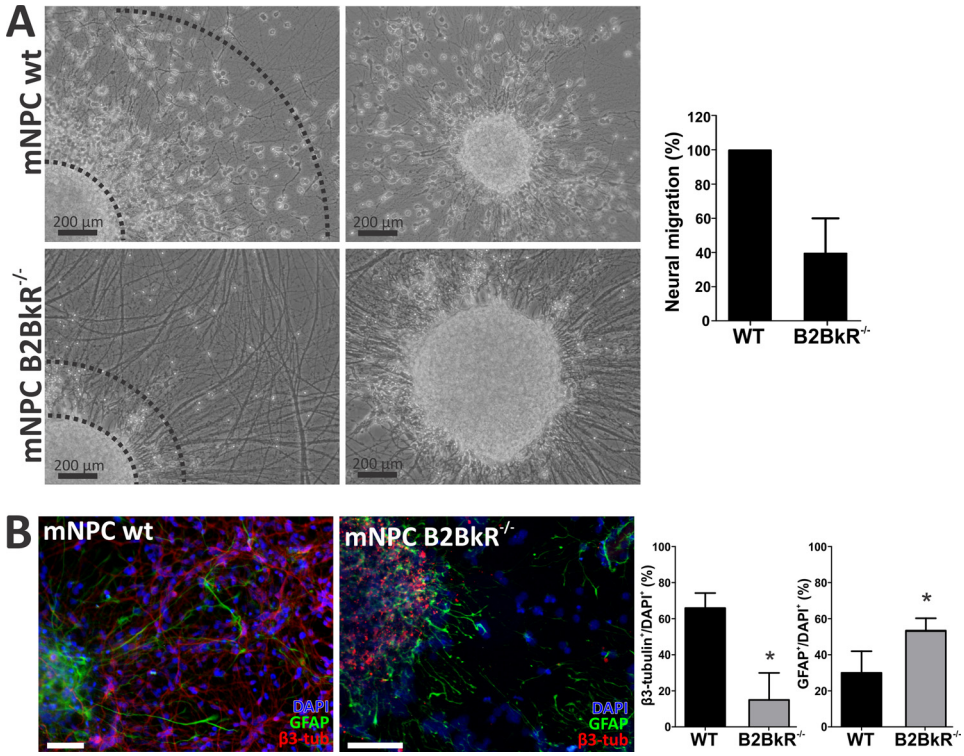

FIGURE 9. **Neural migration and differentiation of neurospheres obtained from *B2BkR*$^{-/-}$ mice.** Differentiation of neurospheres obtained from embryonic telencephalon (*E12.5*) of wild type (*mNPC wt*) and *B2BkR* knock-out mice (*B2BkR*$^{-/-}$ *mNPC*). *A*, phase-contrast images of radial migration pattern after 7 days of neural differentiation. The region enclosed *between the dotted lines* comprises ~95% of cells that migrated. *Scale*, 200 μm ($n = 2$). *B*, immunofluorescence staining of dissociated *B2BkR*$^{-/-}$ mNPC against β3-tubulin and GFAP protein revealed an increase in the number of glial cells compared with wild type mNPC. *Scale*, 20 μm ($n = 2$) (*, $p < 0.05$).

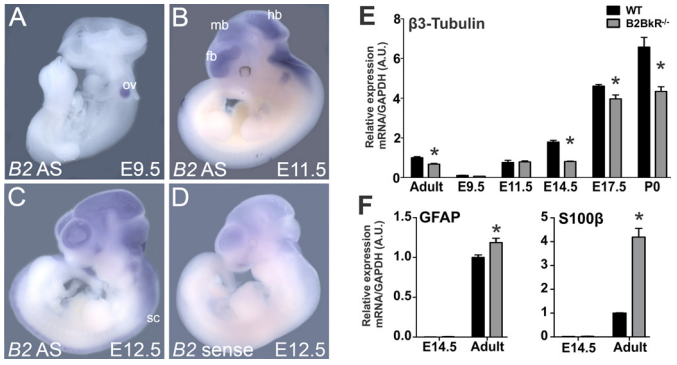

FIGURE 10. **Expression pattern of *B2BkR* during mouse embryo development and neuronal marker expression in telecephalons from *B2BkR* knock-out and wild-type mice.** Whole mount *in situ* hybridization of mouse embryos with *B2BkR* antisense probe (*A–C*) and *B2BkR* sense probe (used as a control, *D*). At stage E9.5, *B2BkR* expression is restricted to the optic vesicle (*A*), strong *B2BkR* expression was observed in the developing nervous system (*B* and *C*), *fb*, forebrain; *hb*, hindbrain; *mb*, midbrain; *ov*, optic vesicle; *sc*, spinal cord. *E*, *β3-tubulin* neuronal marker gene expression during WT and *B2BkR*$^{-/-}$ mouse brain development. The *B2BkR*$^{-/-}$ embryos express less of the marker during several time points of brain development ($n = 6$) (*, $p < 0.05$ by two-way analysis of variance with Bonferroni post-test compared with WT. *Adult*, $p = 0.0334$; *E9.5*, $p = 0.0861$; *E11.5*, $p = 0.4349$; *E14.5*, $p = 0.0004$; *E17.5*, $p = 0.0008$; *P0*, $p = 0.0001$). *F*, *GFAP* and *S100β* glial marker gene expression of WT and *B2BkR*$^{-/-}$ mice brain. Adult *B2BkR*$^{-/-}$ brain reveal more gene expression of glial proteins, such as *GFAP* (*, $p < 0.05$ by two-way analysis of variance, *Adult*, $p = 0.0083$) and *S100β* (*, $p < 0.05$ by two-way analysis of variance, *Adult*, $p = 0.0001$).

its degradation products participate via B1BkR or B2BkR activation in processes similar to those occurring during neurogenesis, such as neurite outgrowth, cell migration, and maturation.

In this context, several other factors can participate in early cell fate determination induced by Bk, including hormones (42) and amyloid-β precursor protein (43). Gallego and co-workers (42) demonstrated that inhibiting hormone signaling prevented the differentiation of embryonic stem cells aggregates into neuroectodermal cells. Porayette and co-workers (43) showed that the inhibition of amyloid-β precursor protein formation significantly suppressed human embryonic stem cell proliferation and promoted NPC formation. Interestingly, there is evidence that sex steroids alter B2BkR expression, and that Bk affects amyloid-β precursor protein processing (44, 45) and increases its secretion. Moreover, due to possible regulation of production and secretion of hormones, growth factors and other substances by Bk, both, direct and indirect effects evoked by this peptide in neural fate determination are possible. In this regard, further investigation of the changes in muscarinic and cholinergic receptor expression and activity in conditions of chronic B2BkR inhibition will provide clues on these mechanisms.

Here we have defined novel functions for Bk and its receptor using rat embryonic telencephalon neurospheres as an *in vitro* model for early cortex neurogenesis and gliogenesis (Fig. 11). Besides intracellular calcium signaling, Bk promotes NO production, essential for the progress of neurogenesis. In agreement with a recently published study of our group, any interference with the production of arginine, the substrate for NO production, or with NOS activity interferes with the differentiation process (30). Subsequently, deficient B2BkR signaling in the presence of HOE-140, resulting in impaired neurogenesis,

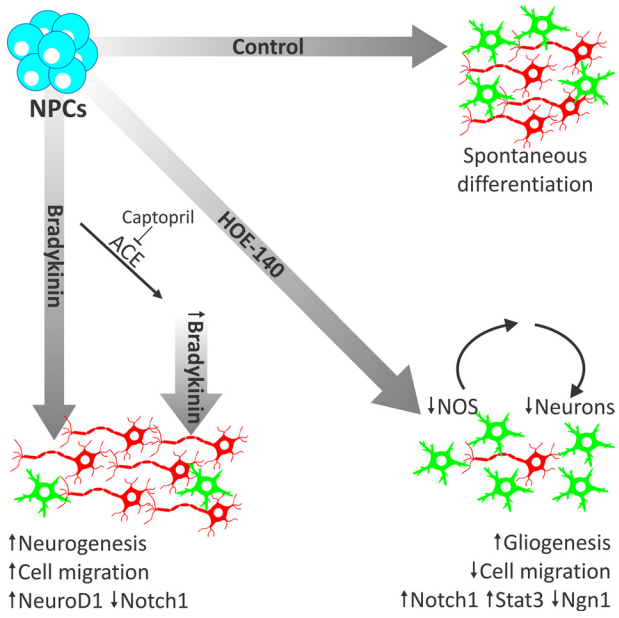

FIGURE 11. **Bradykinin promotes neurogenesis via B2BkR activation.** Following plating, neural stem cells spontaneously differentiate into neurons (*red*) and glial cells (*green*). However, when B2BkR activity is blocked by HOE-140, the progress of neurogenesis is inhibited. The addition of Bk to NPC cultures decreases proliferation and promotes migration and neural differentiation following activation of *NeuroD1* and down-regulation of *Notch1* expression, whereas specific inhibition of the B2BkR reduces neurogenesis and augments gliogenesis following up-regulation of *Notch1* and *Stat3* and down-regulation of *Ngn* (*neurogenin 1*) expression. The increase in neurogenesis of NPCs by Bk is yet enhanced in the presence of captopril, an inhibitor ACE, augmenting the half-time of this peptide in the culture medium. Neurogenic actions exerted by Bk also involved NO production, because expression of key enzymes of the NO-citrulline cycle was down-regulated as result of B2BkR inhibition (30).

is also reflected by down-regulated expression of NOS and the step-limiting enzyme ASS.

B2BkR expression was evident throughout differentiation of neurospheres into neurons and glial cells accompanied by reduction of expression of the neural progenitor marker nestin and an increase in expression of neuronal β3-tubulin and NSE as well as of GFAP and S100β, identifying glial cells. Bk was released into the culture medium during phenotypic transition of undifferentiated cells into specialized neural cells (24). Further evidence for a functional kallikrein-kinin system is given by the expression of ACE, limiting Bk half-life in the extracellular fluid; however, the B1BkR could not be detected, both on expression and activity levels.

These data agree with previous work of our laboratory suggesting the presence of an autocrine loop system of Bk secretion and receptor activation during neuronal differentiation of P19 embryonal carcinoma cells, in which the blockade of receptor activation suppressed Bk liberation into the medium and led to inhibition of *M1–M3 muscarinic receptor* expression in neuronal-differentiated P19 cells (19). Based on these observations during differentiation of an embryonic cell model, we questioned now whether these B2BkR functions are also present in an *in vitro* model closely reflecting conditions occurring during embryonic cortex development in a network of migrating cells.

As found during *in vitro* neurogenesis of P19 cells, gene expression of *M1–M4 receptors* and muscarine-induced $[Ca^{2+}]_i$ transients were reduced following inhibition of B2BkR activity during neurosphere differentiation. Phenotypic changes observed in neurospheres differentiated in the presence of HOE-140 included alterations in purinergic receptor expression and activities. Suppression of *P2X5* and *P2X6* receptor subunit expression, known to be regulated during neuronal development (46), is consistent with an inhibitory effect of B2BkR blockade on the progress of neurogenesis. Scemes *et al.* (47) reported a reduction in neural outgrowth by blocking P2Y1 receptor activity during neurosphere differentiation, whereas the relative population of neurons and glial cells remained unchanged (48). These results are in agreement with the down-regulation of P2Y1 receptor expression due to HOE-140 treatment and subsequent decreased neural migration, agreeing with important roles of this receptor in neural proliferation and migration (49).

There are growing evidence that points at regulatory functions of NO in the development of the CNS, including cell proliferation and fate determination (50–52). The mechanism of regulating proliferation/differentiation depends on the NOS isoform involved in NO production (29). In this context, expression of enzymes of the citrulline-NO cycle including eNOS, nNOS, and argininosuccinate synthetase was also down-regulated in the presence of HOE-140. As a possible mechanism, B2BkR activity controls key events including expression of the machinery necessary for NO formation, which is essential for cell fate determination and guidance of maturation into neurons expressing specific neurotransmitter receptors (50).

Effects of B2BkR inhibition on final neural phenotype determination did not result in increased cell death rate or in the permanence of differentiating cells in the progenitor stage. Moreover, neurogenesis, measured by an increase in the number of β3-tubulin$^+$ cells, augmented with the distance of migration from undifferentiated neurosphere cell aggregates, whereas cells that migrated less showed higher labeling for nestin and GFAP. Therefore, migration is linked directly to neuronal differentiation, and gliogenesis yet occurs due to proliferation of GFAP$^+$ cells. A direct participation of B2BkR in cell migration was confirmed with neurospheres isolated from *B2BkR* knock-out mice, where just as in the presence of HOE-140 migrated distances were reduced. On the other hand, changes in the percentages of β3-tubulin$^+$ and GFAP$^+$ cells induced by chronic treatment with HOE-140 were not observed in primary cultures of postnatal cortex neurons indicating that effects only occur during neural development and not when final neural fate determination and differentiation have already happened.

A possible molecular mechanism for Bk-induced neural fate determination can be delineated by the expression of neural markers and transcription factors related to neurogenesis/gliogenesis switches *in vivo*. Wnt activation in proliferating neural progenitors followed by up-regulation of *Ngn1* expression promotes the expression of genes related to neurogenesis such as *NeuroD1* (53). At the same time, gliogenesis controlled by Ngn1 is induced by activation of Stat3 and expression of GFAP (54). Actually, the cooperation between Smad, Stat, and p300 protein is particularly effective for promoting gliogenesis in NPCs (55, 56). Associated to this molecular machinery, notch 1 regu-

lates interactions between physically adjacent cells and its activation leads to a potent inhibition of neurogenesis, whereas committing the cells to an astrocyte phenotype (57, 58). In this context, activation and inhibition of B2BkR can interfere with the expression and activity of some of these transcription factors, thereby changing cell fate. However, the cause-consequence relationship between B2BkR downstream signaling and the expression of neurogenic genes is not well understood.

Neurogenesis was even more enhanced when Bk was added to the culture medium together with captopril, increasing Bk half-life. In fact, this observation reveals new strategies for strengthening neurogenesis, even in the adult organism following insults like stroke and in neurodegenerative diseases. In view of that, stable B2BkR agonists and ACE inhibitors may gain therapeutic applications for cellular therapy. It is expected that these compounds will also induce endogenous neurogenesis and provide adequate niches for transplanted stem cells to survive.

Less β3-tubulin expression during development of *B2BkR* knock-out animals points to crucial participation of B2BkR during *in vivo* neurogenesis, being in line with previous results showing that neurogenic activities of exogenously added kallikrein or kallikrein gene transfer in an animal model depends on B2BkR activity (59–61). Xia *et al.* (61) suggested that the insertion of tissue kallikrein genes by viral infection in newborn mice promotes ischemic neuroprotection by stimulating glial migration, neurogenesis, and inhibition of apoptosis in the injured area, mainly related to increased levels of phospho-Akt, Bcl-2, and NO, in addition to decreased activation of caspase-3. The observed effects can be explained by the increased availability of Bk and subsequent activation of B2BkR, because they were reversed by pretreatment with HOE-140. Such neuroprotective features were recently described for an *in vitro* model of hippocampal neurons where Bk reversed apoptosis induced by NMDA-mediated excitotoxicity (62).

Bk-induced changes in neural fate determination do not involve alterations in populations of excitatory glutamatergic and inhibitory GABAergic neurons nor of dopaminergic neurons as judged by comparison of global expression levels of neurotransmitters. These results agree with those of calcium imaging assays showing no interference with glutamate receptor activity following chronic treatment with HOE-140 along differentiation. On the other hand, purinergic and muscarinic acetylcholine-receptor expression and activity were affected by the presence of HOE-140. These results are again in line with the suggestion for neurogenic actions of Bk, having in mind that both receptor systems contribute to the progress of neuronal differentiation (63, 64).

França *et al.* (65) showed that expression of B2BkR increases during early rat organogenesis (E8) and stabilizes during fetal growth (E15). Most importantly, besides being strongly expressed in the whole nervous system during the neurogenic stage of embryo development, B2BkR-induced neurogenesis and inhibition of gliogenesis were conserved throughout different models of neurogenesis, even in iPS cells reprogrammed to pluripotency from adult somatic cells. Our work provides new tools for directing differentiating cells into homogeneous populations of neurons *in vitro* for posterior transplantation. In this regard the results obtained with human iPS cells are extremely valuable. In summary, neurogenic properties of Bk described herein may open novel avenues for therapy of neurodevelopmental and neurodegenerative diseases.

REFERENCES

1. Rakic, P. (1988) Specification of cerebral cortical areas. *Science* **241,** 170–176
2. Bayer, S. A., and Altman, J. (1991) *Neocortical Development*, First Ed., Raven Press, New York
3. Noctor, S. C., Martínez-Cerdeño, V., Ivic, L., and Kriegstein, A. R. (2004) Cortical neurons arise in symmetric and asymmetric division zones and migrate through specific phases. *Nat. Neurosci.* **7,** 136–144
4. Pearson, B. J., and Doe, C. Q. (2004) Specification of temporal identity in the developing nervous system. *Annu. Rev. Cell Dev. Biol.* **20,** 619–647
5. Campbell, K. (2005) Cortical neuron specification. It has its time and place. *Neuron* **46,** 373–376
6. Muotri, A. R., and Gage, F. H. (2006) Generation of neuronal variability and complexity. *Nature* **441,** 1087–1093
7. Gross, R. E., Mehler, M. F., Mabie, P. C., Zang, Z., Santschi, L., and Kessler, J. A. (1996) Bone morphogenetic proteins promote astroglial lineage commitment by mammalian subventricular zone progenitor cells. *Neuron* **17,** 595–606
8. Cameron, H. A., Hazel, T. G., and McKay, R. D. (1998) Regulation of neurogenesis by growth factors and neurotransmitters. *J. Neurobiol.* **36,** 287–306
9. Buznikov, G. A., Shmukler, Y. B., and Lauder, J. M. (1996) From oocyte to neuron. Do neurotransmitters function in the same way throughout development? *Cell Mol. Neurobiol.* **16,** 537–559
10. Bhoola, K. D., Figueroa, C. D., and Worthy, K. (1992) Bioregulation of kinins. Kallikreins, kininogens, and kininases. *Pharmacol. Rev.* **44,** 1–80
11. Madeddu, P., Emanueli, C., and El-Dahr, S. (2007) Mechanisms of disease. The tissue kallikrein-kinin system in hypertension and vascular remodeling. *Nat. Clin. Pract. Nephrol.* **3,** 208–221
12. Sainz, I. M., Pixley, R. A., and Colman, R. W. (2007) Fifty years of research on the plasma kallikrein-kinin system. From protein structure and function to cell biology and *in vivo* pathophysiology. *Thromb. Haemost.* **98,** 77–83
13. Walker, K., Perkins, M., and Dray, A. (1995) Kinins and kinin receptors in the nervous system. *Neurochem. Int.* **26,** 1–16; discussion 17–26
14. Raidoo, D. M., and Bhoola, K. D. (1998) Pathophysiology of the kallikrein-kinin system in mammalian nervous tissue. *Pharmacol. Ther.* **79,** 105–127
15. Calixto, J. B., Cabrini, D. A., Ferreira, J., and Campos, M. M. (2000) Kinins in pain and inflammation. *Pain* **87,** 1–5
16. Kansui, Y., Fujii, K., Goto, K., and Abe, I. (2002) Bradykinin enhances sympathetic neurotransmission in rat blood vessels. *Hypertension* **39,** 29–34
17. Eurin, J., Barthélemy, C., Masson, F., Soualmia, H., Sarfati, E., and Carayon, A. (2002) Bradykinin-induced neuropeptide Y release by human pheochromocytoma tissue. *Neuropeptides* **36,** 257–262
18. Wang, H., Kohno, T., Amaya, F., Brenner, G. J., Ito, N., Allchorne, A., Ji, R. R., and Woolf, C. J. (2005) Bradykinin produces pain hypersensitivity by potentiating spinal cord glutamatergic synaptic transmission. *J. Neurosci.* **25,** 7986–7992
19. Martins, A. H., Resende, R. R., Majumder, P., Faria, M., Casarini, D. E., Tárnok, A., Colli, W., Pesquero, J. B., and Ulrich, H. (2005) Neuronal differentiation of P19 embryonal carcinoma cells modulates kinin B2 receptor gene expression and function. *J. Biol. Chem.* **280,** 19576–19586
20. Borkowski, J. A., Ransom, R. W., Seabrook, G. R., Trumbauer, M., Chen, H., Hill, R. G., Strader, C. D., and Hess, J. F. (1995) Targeted disruption of a B2 bradykinin receptor gene in mice eliminates bradykinin action in smooth muscle and neurons. *J. Biol. Chem.* **270,** 13706–13710
21. Negraes, P. D., Schwindt, T. T., Trujillo, C. A., and Ulrich, H. (2011) Neural differentiation of P19 carcinoma cells and primary neurospheres, cell morphology, proliferation, viability and functionality. *Curr. Protoc. Stem. Cell Biol.* **2,** 2D.9
22. Marchetto, M. C., Carromeu, C., Acab, A., Yu, D., Yeo, G. W., Mu, Y.,

Chen, G., Gage, F. H., and Muotri, A. R. (2010) A model for neural development and treatment of Rett syndrome using human induced pluripotent stem cells. *Cell* **143,** 527–539
23. Takahashi, K., Tanabe, K., Ohnuki, M., Narita, M., Ichisaka, T., Tomoda, K., and Yamanaka, S. (2007) Induction of pluripotent stem cells from adult human fibroblasts by defined factors. *Cell* **131,** 861–872
24. Martins, A. H., Alves, J. M., Trujillo, C. A., Schwindt, T. T., Barnabé, G. F., Motta, F. L, Guimaraes, A. O., Casarini, D. E., Mello, L. E., Pesquero, J. B., and Ulrich, H. (2008) Kinin-B2 receptor expression and activity during differentiation of embryonic rat neurospheres. *Cytometry A* **73,** 361–368
25. Schwindt, T. T., Trujillo, C. A., Negraes, P. D., Lameu, C., and Ulrich, H. (2011) Directed differentiation of neural progenitors into neurons is accompanied by altered expression of P2X purinergic receptors. *J. Mol. Neurosci.* **44,** 141–146
26. McLaren, F. H., Svendsen, C. N., Van der Meide, P., and Joly, E. (2001) Analysis of neural stem cells by flow cytometry, cellular differentiation modifies patterns of MHC expression. *J. Neuroimmunol.* **112,** 35–46
27. Henrique, D., Adam, J., Myat, A., Chitnis, A., Lewis, J., and Ish-Horowicz, D. (1995) Expression of a δ homologue in prospective neurons in the chick. *Nature* **375,** 787–790
28. Estrada, C., and Murillo-Carretero, M. (2005) Nitric oxide and adult neurogenesis in health and disease. *Neuroscientist* **11,** 294–307
29. Cárdenas, A., Moro, M. A., Hurtado, O., Leza, J. C., and Lizasoain, I. (2005) Dual role of nitric oxide in adult neurogenesis. *Brain. Res. Brain. Res. Rev.* **50,** 1–6
30. Lameu, C., Trujillo, C. A., Schwindt, T. T., Negraes, P. D., Pillat, M. M., Morais, K. L., Lebrun, I., and Ulrich, H. (2012) Interactions between the NO-citrulline cycle and BDNF in differentiation of neural stem cells. *J. Biol. Chem.* **287,** 29690–29701
31. Hagg, T. (2005) Molecular regulation of adult CNS neurogenesis, an integrated view. *Trends. Neurosci.* **28,** 589–595
32. Ma, D. K., Ming, G. L., and Song, H. (2005) Glial influences on neural stem cell development, cellular niches for adult neurogenesis. *Curr. Opin. Neurobiol.* **15,** 514–520
33. Ghashghaei, H. T., Lai, C., and Anton, E. S. (2007) Neuronal migration in the adult brain. Are we there yet? *Nat. Rev. Neurosci.* **8,** 141–151
34. Purkiss, J., Murrin, R. A., Owen, P. J., and Boarder, M. R. (1991) Lack of phospholipase D activity in chromaffin cells, bradykinin-stimulated phosphatidic acid formation involves phospholipase C in chromaffin cells but phospholipase D in PC12 cells. *J. Neurochem.* **57,** 1084–1087
35. Bush, A. B., Borden, L. A., Greene, L. A., and Maxfield, F. R. (1991) Nerve growth factor potentiates bradykinin-induced calcium influx and release in PC12 cells. *J. Neurochem.* **57,** 562–574
36. Kozlowski, M. R., Rosser, M. P., Hall, E., and Longden, A. (1989) Effects of bradykinin on PC-12 cell differentiation. *Peptides* **10,** 1121–1216
37. Reber, B. F., and Schindelholz, B. (1996) Detection of a trigger zone of bradykinin-induced fast calcium waves in PC12 neurites. *Pflugers. Arch.* **432,** 893–903
38. Lorenzon, P., Zacchetti, D., Codazzi, F., Fumagalli, G., Meldolesi, J., and Grohovaz, F. (1995) Ca^{2+} waves in PC12 neurites. A bidirectional, receptor-oriented form of Ca^{2+} signaling. *J. Cell Biol.* **129,** 797–804
39. Bertram, C. M., Baltic, S., Misso, N. L., Bhoola, K. D., Foster, P. S., Thompson, P. J., and Fogel-Petrovic, M. (2007) Expression of kinin B1 and B2 receptors in immature, monocyte-derived dendritic cells and bradykinin-mediated increase in intracellular Ca^{2+} and cell migration. *J. Leukocyte Biol.* **81,** 1445–1454
40. Lu, D. Y., Leung, Y. M., Huang, S. M., and Wong, K. L. (2010) Bradykinin-induced cell migration and COX-2 production mediated by the bradykinin B1 receptor in glioma cells. *J. Cell Biochem.* **110,** 141–150
41. Yang, W. H., Chang, J. T., Hsu, S. F., Li, T. M., Cho, D. Y., Huang, C. Y., Fong, Y. C., and Tang, C. H. (2010) Bradykinin enhances cell migration in human chondrosarcoma cells through Bk receptor signaling pathways. *J. Cell Biochem.* **109,** 82–92
42. Gallego, M. J., Porayette, P., Kaltcheva, M. M., Meethal, S. V., and Atwood, C. S. (2009) Opioid and progesterone signaling is obligatory for early human embryogenesis. *Stem Cells Dev.* **18,** 737–740
43. Porayette, P., Gallego, M. J., Kaltcheva, M. M., Bowen, R. L., Vadakkadath Meethal, S., and Atwood, C. S. (2009) Differential processing of amyloid-β precursor protein directs human embryonic stem cell proliferation and differentiation into neuronal precursor cells. *J. Biol. Chem.* **284,** 23806–23817
44. Nitsch, R. M., Kim, C., and Growdon, J. H. (1998) Vasopressin and bradykinin regulate secretory processing of the amyloid protein precursor of Alzheimer's disease. *Neurochem. Res.* **23,** 807–814
45. Racchi, M., Ianna, P., Binetti, G., Trabucchi, M., and Govoni, S. (1998) Bradykinin-induced amyloid precursor protein secretion. A protein kinase C-independent mechanism that is not altered in fibroblasts from patients with sporadic Alzheimer's disease. *Biochem. J.* **330,** 1271–1275
46. Burnstock, G., and Ulrich, H. (2011) Purinergic signaling in embryonic and stem cell development. *Cell Mol. Life. Sci.* **68,** 1369–1394
47. Scemes, E., Duval, N., and Meda, P. (2003) Reduced expression of P2Y1 receptors in connexin43-null mice alters calcium signaling and migration of neural progenitor cells. *J. Neurosci.* **23,** 11444–11452
48. Lin, J. H., Takano, T., Arcuino, G., Wang, X., Hu, F., Darzynkiewicz, Z., Nunes, M., Goldman, S. A., and Nedergaard, M. (2007) Purinergic signaling regulates neural progenitor cell expansion and neurogenesis. *Dev. Biol.* **302,** 356–366
49. Ulrich, H., Abbracchio, M. P., and Burnstock, G. (2012) Extrinsic purinergic regulation of neural stem/progenitor cells, implications for CNS development and repair. *Stem Cell Rev.* **8,** 755–767
50. Packer, M. A., Stasiv, Y., Benraiss, A., Chmielnicki, E., Grinberg, A., Westphal, H., Goldman, S. A., and Enikolopov, G. (2003) Nitric oxide negatively regulates mammalian adult neurogenesis. *Proc. Natl. Acad. Sci. U.S.A.* **100,** 9566–9571
51. Gibbs, S. M. (2003) Regulation of neuronal proliferation and differentiation by nitric oxide. *Mol. Neurobiol.* **27,** 107–120
52. Covacu, R., Danilov, A. I., Rasmussen, B. S., Hallén, K., Moe, M. C., Lobell, A., Johansson, C. B., Svensson, M. A., Olsson, T., and Brundin, L. (2006) Nitric oxide exposure diverts neural stem cell fate from neurogenesis towards astrogliogenesis. *Stem Cells* **24,** 2792–2800
53. Ma, Q., Fode, C., Guillemot, F., and Anderson, D. J. (1999) Neurogenin1 and neurogenin2 control two distinct waves of neurogenesis in developing dorsal root ganglia. *Genes Dev.* **13,** 1717–1728
54. Sun, Y., Nadal-Vicens, M., Misono, S., Lin, M. Z., Zubiaga, A., Hua, X., Fan, G., and Greenberg, M. E. (2001) Neurogenin promotes neurogenesis and inhibits glial differentiation by independent mechanisms. *Cell* **104,** 365–376
55. Nakashima, K., Wiese, S., Yanagisawa, M., Arakawa, H., Kimura, N., Hisatsune, T., Yoshida, K., Kishimoto, T., Sendtner, M., and Taga, T. (1999) Developmental requirement of gp130 signaling in neuronal survival and astrocyte differentiation. *J. Neurosci.* **19,** 5429–5434
56. Foshay, K. M., and Gallicano, G. I. (2008) Regulation of Sox2 by STAT3 initiates commitment to the neural precursor cell fate. *Stem Cells Dev.* **17,** 269–278
57. Morrison, S. J., Perez, S. E., Qiao, Z., Verdi, J. M., Hicks, C., Weinmaster, G., and Anderson, D. J. (2000) Transient Notch activation initiates an irreversible switch from neurogenesis to gliogenesis by neural crest stem cells. *Cell* **101,** 499–510
58. Tanigaki, K., Nogaki, F., Takahashi, J., Tashiro, K., Kurooka, H., and Honjo, T. (2001) Notch1 and Notch3 instructively restrict bFGF-responsive multipotent neural progenitor cells to an astroglial fate. *Neuron* **29,** 45–55
59. Ling, L., Hou, Q., Xing, S., Yu, J., Pei, Z., and Zeng, J. (2008) Exogenous kallikrein enhances neurogenesis and angiogenesis in the subventricular zone and the peri-infarction region and improves neurological function after focal cortical infarction in hypertensive rats. *Brain Res.* **1206,** 89–97
60. Xia, C. F., Yin, H., Borlongan, C. V., Chao, L., and Chao, J. (2004) Kallikrein gene transfer protects against ischemic stroke by promoting glial cell migration and inhibiting apoptosis. *Hypertension* **43,** 452–459
61. Xia, C. F., Yin, H., Yao, Y. Y., Borlongan, C. V., Chao, L., and Chao, J. (2006) Kallikrein protects against ischemic stroke by inhibiting apoptosis and inflammation and promoting angiogenesis and neurogenesis. *Hum. Gene. Ther.* **17,** 206–219
62. Martins, A. H., Alves, J. M., Perez, D., Carrasco, M., Torres-Rivera, W., Eterović, V. A., Ferchmin, P. A., and Ulrich, H. (2012) Kinin-B2 receptor mediated neuroprotection after NMDA excitotoxicity is reversed in the

presence of kinin-B1 receptor agonists. *PloS One* **7,** e30755
63. Resende, R. R., Alves, A. S., Britto, L. R., and Ulrich, H. (2008) Role of acetylcholine receptors in proliferation and differentiation of P19 embryonal carcinoma cells. *Exp. Cell Res.* **314,** 1429–1443
64. Resende, R. R., Britto, L. R., and Ulrich, H. (2008) Pharmacological properties of purinergic receptors and their effects on proliferation and induction of neuronal differentiation of P19 embryonal carcinoma cells. *Int. J. Dev. Neurosci.* **26,** 763–777
65. França, C. E., Vicari, C. F., Piza, A. M., Geroldo, E. A., Beçak, M. L., Beçak, W., Stocco, R. C., and Lindsey, C. J. (2010) The kinin B(2) receptor gene structure, product processing and expression in adult and fetal rats. Evidence for gene evolution. *Genet. Mol. Res.* **9,** 215–230
66. Ueno, S., Yamada, H., Moriyama, T., Honda, K., Takano, Y., Kamiya, H. O., and Katsuragi, T. (2002) Measurement of dorsal root ganglion P2X mRNA by SYBR Green fluorescence. *Brain. Res. Brain. Res. Protoc.* **10,** 95–101
67. Lugo-Garcia, L., Filhol, R., Lajoix, A. D., Gross, R., Petit, P., and Vignon, J. (2007) Expression of purinergic P2Y receptor subtypes by INS-1 insulinoma beta-cells. A molecular and binding characterization. *Eur. J. Pharmacol.* **568,** 54–60
68. Bortone, F., Santos, H. A., Albertini, R., Pesquero, J. B., Costa, M. S., and Silva, J. A., Jr. (2008) Low level laser therapy modulates kinin receptors mRNA expression in the subplantar muscle of rat paw subjected to carrageenan-induced inflammation. *Int. Immunopharmacol.* **8,** 206–210
69. Wang, L., Zhang, Z. G., Zhang, R. L., Jiao, Z. X., Wang, Y., Pourabdollah-Nejad, D., LeTourneau, Y., Gregg, S. R., and Chopp, M. (2006) Neurogenin 1 mediates erythropoietin enhanced differentiation of adult neural progenitor cells. *J. Cereb. Blood. Flow. Metab.* **26,** 556–564
70. Zheng, H., Zeng, Y., Chu, J., Kam, A. Y., Loh, H. H., and Law, P. Y. (2010) Modulations of NeuroD activity contribute to the differential effects of morphine and fentanyl on dendritic spine stability. *J. Neurosci.* **30,** 8102–8110
71. Lakner, A. M., Moore, C. C., Gulledge, A. A., Schrum, L. W. (2010) Daily genetic profiling indicates JAK/STAT signaling promotes early hepatic stellate cell transdifferentiation. *World J. Gastroenterol.* **16,** 5047–5056